A Quantitative Tool for Identifying the Epileptogenic Zone using Network Connectivity Analysis

James Michael Gurisko

A Thesis Submitted to the Graduate Faculty of

GRAND VALLEY STATE UNIVERSITY

In

Partial Fulfillment of the Requirements

For the Degree of

Master of Science in Engineering

Padnos College of Engineering

April 2014

Acknowledgments

I would first like to thank my thesis advisor Dr. Robert Bossemeyer for his guidance, expertise, and time commitment throughout this entire project. I would also like to thank my committee members Dr. Samhita Rhodes, Dr. Paul Fishback, and Dr. Konstantin Elisevich for their expertise and guidance. I would like to thank Dr. Elisevich and Spectrum Health for providing exciting and innovative opportunities to the Biomedical Engineering program at Grand Valley State University (GVSU). Thank you to Leah Twilley, a Grand Valley Magazine columnist, for writing and publishing an article about this work and helping to promote the Biomedical Engineering program and research at GVSU. Lastly, I would like to thank my parents Shari Gurisko and Arthur Lack for their continued dedication and support throughout this process.

Abstract

Approximately one-third of patients diagnosed with focal epilepsy do not respond to medication and may be candidates for surgery to remove epileptogenic tissue known as the epileptogenic zone. A detailed pre-surgical evaluation is required and often includes invasive video electroencephalographic monitoring (IVEM) using intracranial surface and depth electrodes, and a camera. The resulting large pools of electrocorticorticographic (ECoG) data are manually analyzed by an expert epileptologist to determine epileptic events. The process is time consuming and prone to human error. This thesis investigates the use of measures to identify the causal relationship between ECoG signals during propagation of a seizure in order to delineate a possible epileptogenic zone. These measures are based on concepts of network connectivity derived from the frequency spectrum of recorded signals called the spectrum-weighted directed transfer function (*swDTF*) and the full-frequency directed transfer function (*ffDTF*). The goal of the thesis is to implement a measure that may aid the surgeon in the decision-making process to optimize the outcome of surgery and possibly minimize the resection volume.

A time-variant adaptive version of both the *swDTF* and *ffDTF* was applied to a simple simulation model. The adaptive *swDTF* achieved higher sensitivity than the *ffDTF* (93% vs. 86%) for the detection of epileptogenicity. Both measures achieved a specificity of 99%. Two time-variant versions of the *swDTF* were compared: 1) an adaptive approach to frequency spectrum estimation using a Kalman filtering algorithm and 2) a short-time spectral estimation approach using overlapping Hamming windows. Each method was successfully applied to a simple simulation model. The measures were then applied to electrodes of clinical ECoG data obtained from Spectrum Health's Epilepsy Monitoring Unit. Sixteen seizures in two patients were analyzed and compared to channels indicated as having seizure activity by the

epileptologist. The adaptive approach was able to identify the electrodes containing seizure activity consistent with expert findings (within 10 mm) in 14 out of 16 (88%) seizures. The short-time approach was able to identify an area within the region of interest (within 30-100mm) as noted by the epileptologist in 12 out of 16 (75%) seizures. The short-time *swDTF* reduced computation time by 95% compared to the adaptive approach. The short-time approach is more susceptible to noise and appears to be less selective whereas the adaptive approach is better able to pinpoint a single channel (± 10 mm). The adaptive measure is preferred due to its robustness to input parameters and ability to pinpoint channels. It is suggested that the short-time approach be used to gain quick insight into the region of interest identified by the 3-10 electrodes with the largest elevated output values and to later isolate single electrodes using the adaptive measure.

Table of Contents

List of Figures

List of Tables

1. Introduction

Epilepsy is one of the most common neurological disorders and affects 65 million people around the world. It is defined as a neurological disorder marked by sudden recurrent episodes of sensory disturbance, loss of consciousness, or convulsions, associated with abnormal electrical activity in the brain. Approximately one-third of patients suffering from epilepsy are diagnosed with refractory epilepsy[1]. Refractory epilepsy is a type of epilepsy that does not respond to anti-epileptic drugs (AEDs). An option for patients suffering from refractory epilepsy is surgery. In several cases, a procedure known as invasive video electroencephalographic (EEG) monitoring (IVEM) is used to locate a possible epileptogenic focus for resection. The electrocorticogram (ECoG) is a derivative of the typical EEG using intracranial electrode arrays implanted on the cortex. The video component of IVEM allows for correlation of events in the ECoG signal with observed clinical symptoms. Typically, the IVEM procedure is performed 24 hours a day for 1 to 14 days. The resulting large pools of ECoG recordings are visually inspected by an expert in epilepsy (epileptologist). This method is time consuming and prone to human error due to the vast amount of data and underlying signal characteristics not apparent by visual inspection. Applying signal processing techniques will not only drastically improve analysis time but may aid the surgeon in the decision process so that the success rate of surgery can be maximized and the volume of resected tissue minimized.

The aim of this thesis is to investigate the application of a quantitative computational technique that could serve as an adjunctive tool for use with visual analysis of the ECoG. The method uses the concepts of network connectivity to explore causal relationships between ECoG signals in the frequency domain. Network connectivity is the idea that information spreads across various functional areas of the brain[2,3]. It is believed that during

an epileptic seizure, epileptic activity begins in a particular region of the brain and spreads across different regions over time. This pattern of propagation can be used to delineate the epileptogenic focus by applying measures of information flow (connectivity). This thesis will employ a multivariate directional connectivity measure known as the time-variant directed transfer function (DTF)[4]. This measure investigates the direct and indirect directional information flow between multiple EEG signals in the frequency domain. Due to the stochastic, non-stationary nature of an epileptic EEG signal, the measure must be repeated over short time duration intervals during which the signal may be considered pseudo-stationary. A normalized version of the time-variant DTF known as the spectrum-weighted DTF (*swDTF*) introduced by van Mierlo et. al[1] is applied in this thesis. The time-variant *swDTF* provides a gauge for the connectivity of a particular site with other sites over the course of an epileptic seizure. The measure can be estimated in a variety of ways. This thesis estimates the time-variant *swDTF* using two different methods: 1) short-time multi-variate autoregressive models (MVAR)[5,6], and 2) adaptive MVAR models using a Kalman filtering algorithm[1,7,8]. The ability and feasibility of the two methods to estimate the time dependent *swDTF* are compared and contrasted.

The methods were validated using large pools of ECoG data provided by Spectrum Health's Epilepsy Monitoring Unit (EMU). The ECoG of two patients suffering from refractory focalized epilepsy was recorded at a sampling rate of 1000Hz for twenty-four hours a day over a two-week period via 72 intracranial electrodes implanted on the cerebrum. The data was annotated by an epileptologist. All recordings, annotations, and other information from the EMU were scrubbed by Spectrum Health to remove all patient information before being obtained. The annotations for each seizure included electrode sites

of interest that were visually considered a candidate for a potential epileptogenic focus. These channels of interest were compared to the potential epileptogenic focus indicated by the resulting time-variant *swDTF* measure for each seizure.

2. Literature Review

2.1 The Electroencephalogram (EEG)

2.1.1 Overview of EEG

Electroencephalography (EEG) indicates the electrical activity of the brain and is considered by many to be the most complex set of signals in nature. This complexity is evident by observing the sample EEG signals shown in Figure 2.1.1. The figure presents a seven channel (channels 38-44 located in the left medial temporal lobe), five second segment of non-epileptic EEG data from the EMU sampled at 1000Hz. For a list of detailed anatomical locations of all electrode numbers mentioned in this thesis, refer to Appendix B. Please note that adjacent channels are likely to be very close to one another in terms of electrode site on the cerebrum. The electrical activity of the brain is the result of ionic current flows throughout the roughly one-hundred billion neurons contained within it[9]. This current is mostly due to a summation of synaptic potentials that conduct to the scalp, and measured with scalp electrodes or the surface of the cortex where they are measured with intracranial electrodes (as in Figure 2.1.1).

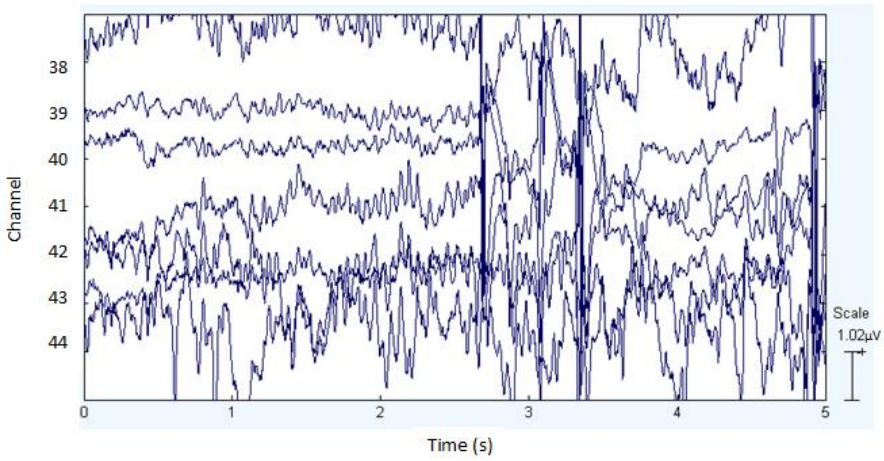

Figure 2.1.1: Electroencephalogram (EEG) Signals

The most common method of recording the EEG is via scalp electrodes arranged in the standard 10-20 placement system as devised by the International Federation of Societies for Electroencephalography due to the non-invasive nature of the procedure. The standard 10-20 placement system[9] of electrodes is shown in Figure 2.1.2 below.

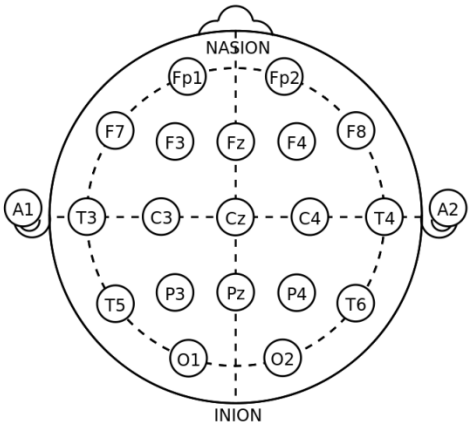

Figure 2.1.2: 10-20 Placement System for EEG

Scalp EEG recordings suffer from two major problems: 1) source localization and 2) presence of artifacts. Because potentials underlying the EEG are generated predominately on the surface of the cortex and propagated to the scalp surface for measurement, the signal at the surface is the summation of many synaptic potentials. One surface electrode may detect the activity of up to a billion cortical neurons[9]. This makes it extremely difficult to pinpoint the exact source of a particular signal of interest. The presence of artifacts is also a major problem because scalp potentials are very low amplitude, only ranging from 10μV to 100μV. These small amplitudes are easily influenced by muscular and ocular artifacts. Muscle artifacts are due to the electrical activity of the muscles and are a result of muscle contractions. These muscle artifacts have amplitude approximately ten times that of the EEG. Ocular artifacts are due to the

electrical activity of the eyes and although they have a lower amplitude than the EEG they can still influence the signal, particularly during blinking of the eyes.

Another option for recording the EEG is via intracranial electrode arrays placed directly on the cerebral cortex. This type of EEG is referred to as the electrocorticography (ECoG) and involves a highly invasive procedure. The primary benefit of ECoG over scalp EEG is the ability to record electrical activity much closer to the source. This essentially eliminates the source localization problem and susceptibility to noise artifacts discussed above. Another benefit is the large increase of signal strength with respect to noise and artifacts as the signals do not have to propagate through the many layers separating the cortex and scalp (i.e., on-site surveillance).

2.1.2 Clinical Use of EEG

The EEG has been used clinically for nearly 80 years since its origination by Hans Berger, a German psychiatrist, in 1924. Since its introduction, little has changed conceptually about the EEG aside from experience, recording hardware, and the speed and power of the computational tools used to analyze it. EEG signals have been used to investigate many neurological diseases including sleep disorders, psychological disorders, cerebrovascular lesions, tumors, and epilepsy[9,10]. Due to the non-stationary, chaotic, and non-linear nature of the EEG, gaining information by direct visual analysis is very difficult and advanced signal processing techniques can provide significant insight. Although the EEG appears random in nature, it contains useful information regarding the state of the brain and thus has clinical value.

2.2 Epilepsy

2.2.1 Seizure

The Epilepsy Foundation reports that 1 in 10 Americans have had a seizure[11]. A seizure is caused by abnormal electrical activity in the brain, specifically excessive synchronous neuronal activity[12]. An example of this excessive synchronous activity can be seen in channels 38-42 shown in Figure 2.2.2. This figure shows a five second segment of channels 38-44 recorded in the EMU during an epileptic seizure. Note that not all channel exhibit this synchronicity (channels 43 and 44 on grid E in the subtemporal region in Figure 2.2.2) as not all parts of the brain are being affected by this particular seizure. The brain is controlled by a series of chemical reactions that result in excitatory or inhibitory discharges. When the balance of these discharges is moved too far toward an excitatory level, a seizure can occur.

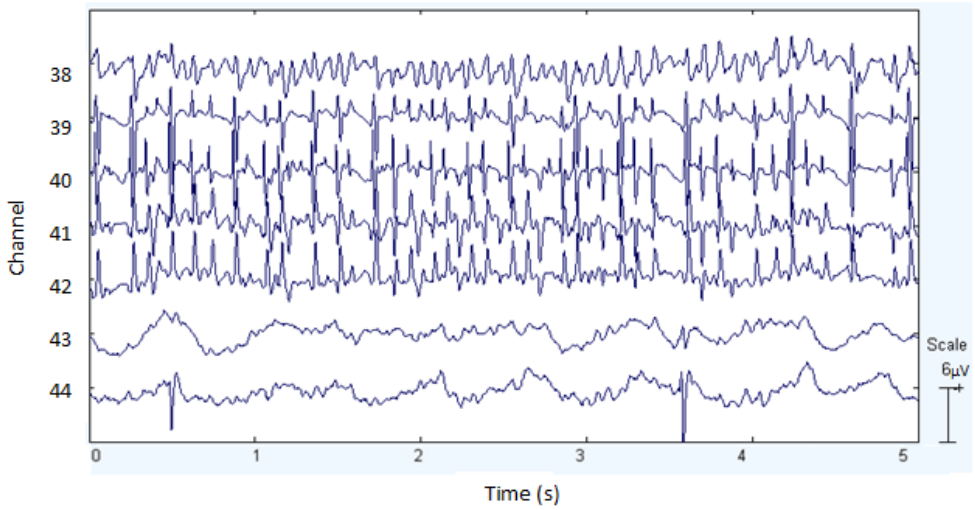

Figure 3.2.2: Abnormal Synchronous EEG Activity during Seizure

There are two main categories of seizures: 1) partial (focal) and 2) generalized[12]. A simplified version of the international classification of seizures is shown in Table 2.2.1

below. It is important to note that the site of abnormal electrical discharges determine the effect the seizure has on the patient.

Table 4.2.1: Classification of Seizures

Partial (Focal) Seizures
Start at particular focal point in cortex
Sensory (e.g., phantom smells)
Motor (e.g., twitching)
Sensory-Motor
Memory
Generalized
Start on both sides of brain
Absence (petit mal)
Sluggish, sleepy, confused
Tonic-Clonic (grand mal)
Loss of consciousness, Stiffening (tonic) followed by jerking (clonic)
Secondarily Generalized
Partial (Focal) seizure that spreads into generalized

A Partial or Focal seizure occurs in a particular location of the cortex. If the seizure occurs in the motor cortex, the patient may experience jerking or stiffening. Seizures occurring in the cortex serving sensory appreciation may result in phantom smells, visual changes, and tactile sensations. In contrast, generalized seizures typically involve the entire brain and may lead to loss of consciousness and tonic-clonic behavior. A seizure may begin as a focalized seizure and spread to the rest of the brain, resulting in a tonic-clonic seizure. This is known as a secondarily generalized seizure.

The physiologic state of a seizure is referred to as the “ictus” or “ictal” period. Consequently, the time periods immediately before, during, and after a seizure are

respectively denoted as the pre-ictal, ictal, and post-ictal periods. The period between seizures is referred to as the inter-ictal period wherein sporadic discharges provide a signature of anomalous behavior.

2.2.2 Epilepsy

The terms epilepsy and seizure are often and incorrectly used interchangeably. It is important to note that a seizure is a *symptom* of epilepsy and that one seizure is not considered epilepsy. Epilepsy is a chronic neurological disorder characterized by the manifestation of hypersynchronous neurological firing resulting in recurrent and spontaneous epileptic seizures[12,13]. Epilepsy symptoms and etiology differ for each individual and, similar to a seizure, epilepsy can be referred to as partial (focal), generalized, or secondarily generalized. In the case of partial (focal) epilepsy, the region of the brain generating the epileptic seizures is termed the epileptogenic zone[12].

According to the Epilepsy Foundation, epilepsy is the fourth most common neurological disorder in the U.S. behind migraine, stroke, and Alzheimer's disease[11]. Epilepsy affects 2.2 million Americans and 70 million people worldwide with 45 people per 100,000 developing new-onset epilepsy each year[14].

2.2.3 Epilepsy Surgery

The prognosis of epilepsy is generally good. Approximately two-thirds of patients are rendered seizure free by treatment with antiepileptic drugs (AEDs). Although the number of AEDs is growing, one-in-three of those diagnosed do not respond to AEDs and continue to experience seizures with varying degrees of frequency and severity[14]. These patients suffer from refractory epilepsy. Commonly used options for treating those suffering from refractory epilepsy include vagus nerve stimulation,

deep brain stimulation, the ketogenic diet, and epilepsy surgery[13,14]. Epilepsy surgery can be divided into two different procedures: 1) resective surgery leading to complete removal of the epileptogenic focus or 2) disconnective surgery leading to cutting of nerve bundles to prevent spreading of seizure activity[13].

Only a few thousand epilepsy surgeries are performed each year due to limitations in knowledge regarding the root cause of epilepsy, availability of resources, cost, and strict criteria[14]. Common criteria that must be met by candidates for epilepsy surgery according to the Epilepsy Foundation are summarized in Table 2.2.2[11].

Table 5.2.2: Epilepsy Surgery Candidate Criteria

Criteria
Diagnosis of epilepsy is secure
Failure of at least two AEDs in controlling seizures
Onset site can be localized (Focal epilepsy)
Epileptogenic Focus can be safely removed
Understanding of benefits/risks and desires surgery

Localizing the epileptogenic focus is a difficult task. A variety of modalities are used including magnetic resonance imaging (MRI), positron emission tomography (PET), and EEG[14]. MRI provides a structural image of the brain and can show underlying causes of seizures including abnormal blood vessels, tumors, etc.. PET shows glucose consumption of the brain. The region of the brain that includes the epileptogenic focus often shows low glucose consumption[14]. EEG is the most commonly used technique because of its availability and ability to monitor the electrical activity of the brain. The presence of abnormal electrical activity is important in determining the epileptogenic focus[14]. An important technique involving EEG is known as invasive

video-EEG monitoring (IVEM). Thin contacts and wires organized into strips or grids are inserted (intracranially) into a region of the brain that is suspected to contain the epileptogenic focus. These may be on the surface of the cortex or within deeper layers (depth electrodes). Patients are monitored in a hospital epilepsy monitoring unit (EMU) from 5 to 14 days and are gradually weaned off their anti-epileptic medication in order to provoke seizures for recording purposes.

The resulting large pools of intracranial EEG data are visually analyzed by an expert in epilepsy (epileptologist) and the epileptogenic focus is delineated. Memory and psychological tests are performed as well as MRI or CT scans to determine if the epileptogenic focus can be removed (or even reached) without severe loss of function. Upon completion of the pre-surgical evaluation, discussion between patient and doctor ultimately determines whether to proceed with surgery.

The outlook after epilepsy surgery is generally good but there is certainly room for improvement. According to the Epilepsy Foundation, a study published in the New England Journal of Medicine showed that after 1 year, 58% of patients who had undergone surgery had not experienced a seizure that impaired consciousness and 38% had not experienced any seizure[11].

2.3 Signal Modeling

2.3.1 Multivariate Autoregressive Modeling (MVAR)

Signal modeling is a way to represent a signal via model parameters that can be used to reveal information (for prediction, reconstruction, etc.) that is not apparent in the current state of the signal. The autoregressive model (AR) is a generic model that is used to represent a time series of signal samples, specifically time-varying processes in nature

such as the EEG. An autoregressive model of order p expresses an N point time series $y(n)$ as a linear combination of past observations $y(n-k)$and white noise $e(n)$,

$$y(n) = \sum_{k=1}^{p} a_k y(n-k) + e(n) \qquad \text{(Eq. 1)}$$

where $a_k$is the k^{th} autoregressive coefficient. The model order p is also referred to as the maximum delay or lag of the model as it determines the number of past samples used in modeling the signal. The parameters of the AR model can be estimated by methods such as Yule-Walker or Least Squares[15].

The AR model can be extended to a multivariate case consisting of M time series, $y_m(n) = \{y_1(n), \dots, y_M(n)\}$. This is known as the multivariate autoregressive model (MVAR) and is defined as:

$$\begin{bmatrix} y_1(n) \\ \vdots \\ y_M(n) \end{bmatrix} = \sum_{k=1}^{p} A_k \begin{bmatrix} y_1(n-k) \\ \vdots \\ y_M(n-k) \end{bmatrix} + \begin{bmatrix} e_1(n) \\ \vdots \\ e_M(n) \end{bmatrix} \qquad \text{(Eq. 2)}$$

where $A_k$is the M by M autoregressive coefficient matrix for order k[7]. The MVAR model is time-invariant and assumes stationary and constant interactions between signals over time. This is not the case of the EEG, especially during an epileptic seizure. A time-varying MVAR model must be generated in order to effectively model these signals.

2.3.1.1 Adaptive Multivariate Autoregressive Models

The MVAR model can be adapted for use with non-stationary multivariate time series by allowing the autoregressive coefficient matrices A_k to vary in time (i.e., $A_k \rightarrow A_k(n)$) where

$$A_k(n) = \begin{bmatrix} a_{11}^k(n) & \cdots & a_{1M}^k(n) \\ \vdots & \ddots & \vdots \\ a_{M1}^k(n) & \cdots & a_{MM}^k(n) \end{bmatrix}. \quad \text{(Eq. 3)}$$

This time-varying extension of the MVAR is known as the adaptive MVAR model. The methods for estimating parameters of the AR model mentioned earlier (Yule-Walker and least squares) are not appropriate in this multivariate adaptive case because there exist more unknown parameters than data points[13]. One way to estimate these coefficients is by using a Kalman filtering algorithm.

The Kalman algorithm represents a signal model in state-space form. This model consists of a state equation and an observations equation. The observations equation is given in Eq. 1 and the state equation is simply stated as:

$$A_k(n) = A_k(n-1) + V_k(n-1) \quad \text{(Eq. 4)}$$

where V_k is the covariance matrix of process noise w_k[8]. The state-space equations are solved using a recursive prediction algorithm followed by an update step[4]. The update step is controlled by the update coefficient (UC). The UC is a constant value set a priori and ranges from 0 to 1. The larger the value of the UC, the quicker the model adapts to changes in the data. The lower the UC, the more robust the estimate[13]. The resulting adaptive MVAR model is capable of simultaneous modeling of extremely non-stationary components of a signal, including the collection of signals that are the EEG electrode recordings.

2.3.1.2 Short-Time Multivariate Autoregressive Models

Estimating an adaptive MVAR model via the Kalman filtering algorithm is a complicated and computationally intensive approach that may be considered overkill

in some cases, especially when dealing with signals that may be considered stationary over short periods of time. In these cases, a short-time (ST) MVAR model using the short-time Fourier transform (STFT) may be appropriate. This method has been successfully applied to newborn EEG signals to calculate time-varying cortical neural connectivity[5]. When computing a STFT, a symmetric sliding window is used to reduce spectral leakage at the edges of the signal (i.e., edge effect). Most often, bell shaped windows such as Hamming or Blackman are employed. The windows will often overlap by 50% when sliding to yield better time-frequency resolution. The ST-MVAR model is computed by dividing each signal $y_k(n)$ into short overlapping segments that are then windowed using the Hamming window. The signal is assumed stationary within the short window and the time-invariant MVAR coefficient matrices $A_k$are estimated within the window.

Due to the nature of the windowing approach, the smoothness and continuity of connectivity measure derived from the short-time approach are inferior to that of the adaptive approach[5]. This is because the measure is only estimated one time within the window using the short-time approach instead of being estimated at every time point using the adaptive approach. Because of the delay that is inherent in the Kalman filtering algorithm as a result of the updating step, the short-time approach is able to more accurately localize events in time. The major drawback of the ST-MVAR approach is the assumption of a stationary signal within the window, which may not be the case[5].

2.4 Network Connectivity

2.4.1 Overview of Network Connectivity

The idea that different brain functions are achieved by communicating across, and interacting with, various regions (areas) of the cerebral cortex is known as network connectivity or brain connectivity. Assessing network connectivity allows one to measure this integration of cerebral areas in the brain. Network connectivity can be divided into three different groups: structural, functional, and effective connectivity[2]. A summary of the three groups is provided in Table 2.4.1 and Figure 2.4.1.

Table 6.4.1: Types of Network (Brain) Connectivity

Connectivity	Definition	Examining Modalities
Structural	Connectivity between fiber pathways tracking over regions of the brain	Magnetic Resonance Imaging (MRI), Diffusion Tensor Imaging (DTI)
Functional	Temporal correlations among different neural areas, dependence between brain regions	EEG, Local Field Potentials (LFP), Magnetoencephalography (MEG), Positron Emission Tomography (PET), Functional MRI (fMRI)
Effective	Direct or indirect influence that one neural system exerts over another	Estimated directly from signals (data-driven), based on models specifying causal linkage

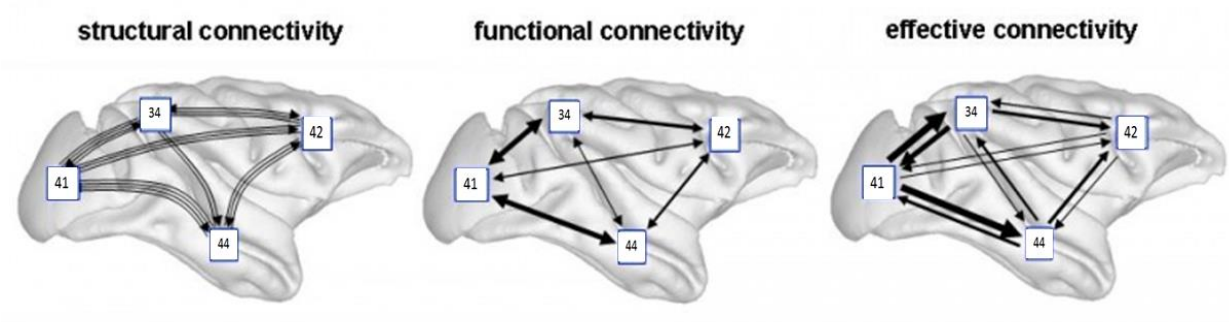

Figure 7.4.1: Network (Brain Connectivity Diagrams)[2]

Figure 2.4.1 shows a graphical representation of the three types of connectivity. The numbers in the boxes represent electrode sites corresponding to EEG signal traces. The arrows represent the connectivity pattern between the various electrode sites (in this example, electrodes 34, 41, 42, and 44).

Structural connectivity is very difficult to calculate due to the dynamic nature of synaptic interactions (i.e., the number and connections of neurons are constantly changing in the brain). Techniques such as the EEG are ideal for estimating functional and effective connectivity because of the high temporal resolution[2]. Since the EEG can be recorded at high sampling frequencies (in this case 1000Hz), the direction of information exchange and movement via functional and effective connectivity within the brain can easily be traced over time by analyzing delays between electrodes. This is useful when investigating the direction of communication between neural signals.

2.4.2 Measures of Network Connectivity

Network connectivity has been investigated since the early 1960s but effectively and accurately quantifying this connectivity remains a problem[2]. Because of this, many methods have been developed to quantify both effective and functional connectivity. One of the original techniques for estimating effective connectivity is Granger-causality (GC). GC is a data-driven technique because it does not assume any prior knowledge or underlying model to estimate the connectivity. The measure is based on the idea that causes precede effects in time[2]. Essentially, a signal x Granger-causes (or G-causes) a second signal y if y can better be predicted using past information from x than past information from y alone[13,2].

GC is a time-domain measure initially developed by Granger in 1969 to analyze the relationships underlying econometric models[16]. Granger-causality has more recently become popular in neuroscience following the development of the spectral G-causality using Fourier methods by Geweke in 1982[17]. Intuitively, spectral GC measures the fraction of total power at a particular frequency of y that is contributed by x. Spectral Granger-causality has led to the development of closely related alternative measures such as the partial directed coherence (PDC)[18] and the directed transfer function (DTF)[19], both of which have been used in regards to epilepsy and delineating the epileptogenic focus[18,19]. These methods are discussed in the following sections.

2.4.2.1 Partial Directed Coherence

The Partial Directed Coherence (PDC) is a derivative of the most commonly used connectivity measure, coherence. Coherence was introduced in 1968 to estimate connectivity between EEG signals[20]. Coherence can be used as a measure of the consistency (or synchronization) of phase angles between two signals and can be loosely considered as a frequency-domain equivalent to cross-correlation[13,21].

One of the major problems with coherence is that it is only a bivariate measure (it is only capable of considering two signals at a time). When analyzing information flow in the brain, it is important to consider all channels at once using a multivariate measure. The Partial Coherence (PC) is a multivariate extension of coherence that differentiates between direct and indirect relationships between signals by removing the influence of all other channels in the system[13,18].

Yet another problem present in both the coherence and partial coherence is the lack of directionality. In other words, coherence and PC only describe mutual synchronicity between signals and do not reveal the direction of the information flow.

This led to the development of the partial directed coherence which considers the temporal relationship (i.e., the time delay) between signals in order to reveal the direction of information flow[18].

2.3.2.2 Directed Transfer Function (DTF)

The Directed Transfer Function (DTF) is a multivariate, directed measure capable of extracting the directional information flow between various signals[22]. The DTF has been shown to be a multivariate frequency domain equivalent to Granger causality[6]. The spectral transfer function $H(f)$ of an autoregressive modeled signal $y(n)$ is computed by taking the inverse of the Fourier transformed MVAR coefficients,

$$H(f) = A^{-1}(f), \quad \text{where } A(f) = -\sum_{k=0}^{p} A_k e^{-i2\pi fk} \qquad \text{(Eq. 5)}$$

and $A_0$is equal to the M by M identity matrix[13,6]. The transfer function can be extended to the multivariate time-variant case by computing Equation 5 for the multivariate adaptive or short-time coefficients $A_k(n)$. The resulting transfer function is of the form $H_{i_j}(f,t)$ and represents the connection between the $i^{th}$and j^{th} signals at frequency f and time t. The time-variant directed transfer function is the square of the absolute values of $H_{i_j}(f,t)$ and may be normalized with respect to the incoming information flow:

$$DTF_{ij}(f,t) = \frac{\left|H_{ij}(f,t)\right|^2}{\sum_{z=1}^{M}|H_{iz}(f,t)|^2}. \qquad \text{(Eq. 6)}$$

Thus, $DTF_{ij}(f,t)$ represents the causal information flow from signal j to signal i at frequency f and time t. The values of the time variant DTF range from [0, 1]. A

value of 1 indicates that all of signal i is the result of information flowing from signal j at that particular frequency and time. A value of 0 indicates that no flow of information is occurring from signal i to signal j at that particular time and frequency[13].

2.3.2.3 Full-frequency & spectrum-weighted DTF (*ffDTF & swDTF*)

One problem present in the adaptive DTF (*ADTF*) and the short-time DTF (*ST-DTF*) is that neither measure takes into account the power spectrum of the signals. This means that each frequency considered in the measure is equally important. Prioritizing frequencies by their power is useful for identifying those frequencies playing an important role in the signal. This led to the introduction of the full-frequency directed transfer function (*ffDTF*) by Korzeniewska[23]. The *ffDTF* can be time invariant (*ffDTF*), adaptive (*ffADTF*), or short-time (*ffST-DTF*) depending on the type of MVAR model used to fit the data. Each time point of the time-variant DTF is normalized by the frequency content in the frequency band considered $[f_1, f_2]$:

$$ffDTF_{ij}(t) = \frac{\sum_{f=f_1}^{f_2} |H_{ij}(f,t)|^2}{\sum_{z=1}^{M} \sum_{f=f_1}^{f_2} |H_{iz}(f,t)|^2} \quad \text{(Eq. 7)}$$

The sum of incoming information flow into a channel from all other channels at a particular time is equal to one[13,23].

A problem present with the ffDTF is the tendency for $H_{ij}(f,t)$ to be high when there is no power in the spectrum of the sending signal. This led to the introduction of the spectrum-weighted directed transfer function (*swDTF*) which is a modified

version of the ffDTF weighted by the autospectrum of the sending signal, j[1]. The time-variant *swDTF* is defined as:

$$swDTF_{ij}(t) = \frac{\sum_{f=f_1}^{f_2} \left|H_{ij}(f,t)\right|^2 \sum_{z=1}^{M} \left|H_{jz}(f,t)\right|^2}{\sum_{l=1}^{M} \sum_{f'=f_1}^{f_2} |H_{il}(f',t)|^2 \sum_{s=1}^{M} \left|H_{js}(f',t)\right|^2}. \quad \text{(Eq. 8)}$$

As with the *ffDTF*, the *swDTF* is normalized so that the sum of incoming information flow into a channel at a particular time point is equal to 1. The *swDTF* additionally weights outgoing information by the autospectrum of the sending signal, j.

All methods and concepts discussed in this literature review will be applied to clinical ECoG data to quantify the location of the epileptogenic zone according to the specific aims of the thesis discussed in the following section.

3. Specific Aims

Visually analyzing the large pools of ECoG data recorded during an video electrocorticographic monitoring procedure (IVEM) is problematic for reasons including analysis time and accuracy. This thesis introduces a computational technique that can be used as an adjunctive tool to alleviate these problems. The computational tool is an automated algorithm which uses network connectivity measurements, specifically the time-variant spectrum-weighted directed transfer function (*swDTF*), to delineate the epileptogenic focus. The process can be broken down into six steps: 1) normalization and extraction of segment of epileptic ECoG data 2) fitting of multivariate autoregressive model (MVAR) for extracted data 3) estimation of time-variant transfer function from MVAR coefficients 4) normalization of time-variant transfer function to estimate time-variant *swDTF* 5) setting of uniform threshold (99.9 percentile of *swDTF* values) to determine significant values of time-variant *swDTF* and 6) generation of "connectivity histogram" by summing across time and outgoing information flow. The channel with the largest histogram value may be indicative of the epileptogenic focus for the particular seizure.

Two methods for estimating the time-variant MVAR model will be utilized and compared: 1) short-time MVAR model and short-time *swDTF* (*swST-DTF*) using overlapping hamming windows and 2) adaptive MVAR model and adaptive *swDTF* (*swADTF*) using a Kalman filtering algorithm. The methods are first compared and verified using a simple simulation model consisting of four channels (simulating four electrodes). At a particular time, a non-stationary sinusoid buried in uncorrelated white noise begins in a particular channel and later spreads to other channels in the model. The simulation is expanded to sixteen channels and the methods will again be verified. The sensitivity and

specificity of the connectivity measures for the simulation will be calculated by comparing the intrinsic connectivity of the simulated model at each time point with the calculated connectivity. The sensitivity is the ability of a measure to identify positive results (e.g., when there is a connection) and the specificity is the ability of a measure to identify negative results (e.g., when there is no connection)[13]. These statistical measures are defined in equations 9 and 10.

$$sensitivity = \frac{True\ Positives}{True\ Positives + False\ Negatives} \quad \textbf{(Eq. 9)}$$

$$specificity = \frac{True\ Negatives}{True\ Negatives + False\ Positives} \quad \textbf{(Eq. 10)}$$

The measures will then be applied to ECoG data of two patients from Spectrum Health's Epilepsy Monitoring Unit (EMU). Both the swADTF and swST-DTF will be applied to each seizure for each patient. The output of each measure will be displayed in two ways: 1) a histogram showing the total reinforcements over time of all connections from a particular channel to all other channels and 2) an image plot showing the relationship (i.e., reinforced connections over time) between each pair of channels as a heat map (red color indicates strong connected relationship from a signal *j* to a signal *i*, blue indicates week connected relationship from a signal *j* to a signal *i*). The channel with the highest histogram value is the channel that is influencing (i.e., connecting with) other channels the most during onset of the seizure and is indicative of the epileptogenic focus. The results will be compared to channels of interest noted by the expert epileptologist.

4. Methodology

4.1 Software Overview

The software implemented in this thesis is performed in three major steps: 1) Fitting of time-variant MVAR model to simulated or clinical ECoG data and obtaining the time-variant frequency domain transfer function 2) Normalization of transfer function to obtain time-variant *swDTF* and 3) Thresholding *swDTF* values and summing over time to determine the total reinforcements of a connection caused by a channel (displayed as a histogram). The methods were applied to both a simple simulation model and ECoG data recorded in the EMU. All customized software was written in the MATLAB R12 (Mathworks, Natick, MA) environment. The open-source package EEGLAB was used to import, manage, and display the ECoG recordings. EEGLAB was developed by the Swartz Center for Computational Neuroscience (SCCN) and is distributed under the GNU General Public License. The BioSig toolbox is an open source software library for biomedical signal processing and is also distributed under the GNU General Public License. Some functions implemented in the BioSig toolbox for MATLAB were used to generate the MVAR coefficients using a multidimensional Kalman filter algorithm.

4.2 Generating Model

4.2.1 Adaptive Approach

The MVAR model is the first major signal processing step performed. The time-variant coefficients of the MVAR model are generated using the *mvaar()* function from the BioSig toolbox. The *mvaar()* function estimates the MVAR model based on a multidimensional Kalman filter algorithm. An optimal order of $p=10$ for the MVAR model was determined using the ARFIT MATLAB package. The ARFIT MATLAB package estimates parameters for MVAR models using an empirical approach that

determines optimal model order by minimizing error in the model[24]. The update coefficient (UC) of the Kalman algorithm was set to *UC = 0.001* as recommended by literature and the *mvaar()* function[13].

The time-variant frequency domain transfer function from channel *j* to channel *i* at time *t* and frequency *f*, $H_{i_j}(f,t)$ was obtained from the MVAR coefficients $A_k(n)$ using Equation 5. The Fourier Transform was computed from 1-30Hz over *N=30* bins, providing a frequency resolution of 1Hz. These numbers are consistent with recommendations in the literature[1,5,7,13].

4.2.2 Short-Time Approach

The time-variant MVAR coefficients are generated by dividing the signal of interest into short segments, windowing each segment by a Hamming window, and computing time-invariant MVAR coefficients within the window. The signal is assumed stationary within the window. The time-invariant coefficients were estimated using the *mvar()* function included in the BioSig toolbox. The *mvar()* function computes the MVAR coefficients using a Nutall-Strand unbiased partial correlation estimation[24]. The window length was empirically chosen to be 100ms as it proved to offer the best balance between temporal and frequency resolution after varying the window size from 50-1000ms. The 100ms windowed segments overlapped by 50%. The window is shifted and the time-invariant MVAR coefficients are calculated within each window. This collection of time-invariant MVAR coefficients is used to compute the time-variant transfer function $H_{i_j}(f,t)$ in the same manner described in the previous section. The only difference is that the time variable *t* represents the transfer function value for the 50ms time window instead of the individual time point in the adaptive case.

4.3 Obtain time-variant *swDTF* Output

The time-variant $swDTF_{ij}(t)$ from channel *j* to channel *i* at time *t* was calculated by normalizing the values of the transfer function $H_{ij}(f,t)$ using Equation 8 over a frequency range of 5-30 Hz as recommended in the literature[13]. A threshold was chosen by finding the 99.9 percentile of all $swDTF_{ij}(t)$. This threshold was used to determine significant connections by comparing the value of $swDTF_{ij}(t)$ at each *t* to the threshold. If the value $swDTF_{ij}$ at time *t* exceeds the threshold, a significant connection is recorded from channel *j* to channel *i* at that time *t*. This method is repeated across all time *t* to determine the "reinforcements of connections" between channels *j* and *i*. The "reinforcements of connections" therefore equals the number of computed $swDTF_{ij}$ values that exceeded the 99.9 percentile threshold across all time *t*. Please note that the threshold used to calculate the number of "reinforcements of connections" for each measure is calculated using the values of that particular measure (e.g., the threshold for the short-time *swDTF* is based off of values of the short-time *swDTF*). While this method does mean that there will always be at least one significant connection, it is important to clarify that the primary interest is in the channels with the most significant connections rather than the total number of significant connections. The number of reinforcements of that connection was summed across all time and all receiving channels *i* for each sending channel *j*. This shows the total number of reinforcements of a connection over time a particular channel *j* is causing.

The output is plotted as a series of two plots. The first plot is a histogram showing the sending channel *j* on the x-axis and the total number of reinforcements of connections to all other channels *i* over all time *t* on the y-axis. The second plot is a heat-map style image plot which shows the relationship between each pair of channels over all time. Each pixel

represents a relationship between a pair of channels with the sending channel *j* on the x-axis and the receiving channel *i* on the y-axis. This plot provides insight into which areas of the brain the sending channel is influencing (causing the most connections in) rather than simply the total number of reinforcements of a connection a channel is causing in all other channels. The sending channel *j* with the largest histogram value is indicative of a region that may be highly epileptogenic.

4.4 Simulation Model

A simulation model was generated to test the time-variant $swDTF$ methods. The results using the adaptive and the short-time approach were compared. The model was also used to compared the *ffADTF* (Eq. 7) and the *swADTF*. The sensitivity (Eq. 9) and specificity (Eq. 10) were calculated for each method.

The simulation model consists of four signals representing four electrodes in the brain. At time t=0s, a non-stationary (12Hz at t=0s decreasing to 8Hz at t=3s) sinusoid with 5dB signal to noise ratio (SNR) begins in channel 1 of the simulation model. Prior to time t=0s, all channels contain uncorrelated white noise. At time t=125ms, the signal is passed from channel 1 to channel 2. At time t=250ms, the signal was passed from channel 2 to channel 3. And at time t=375ms, the signal was passed from channel 2 to channel 4. The simulation model is shown below in Figure 4.4.1 and is described in further detail by van Mierlo et. al[13].

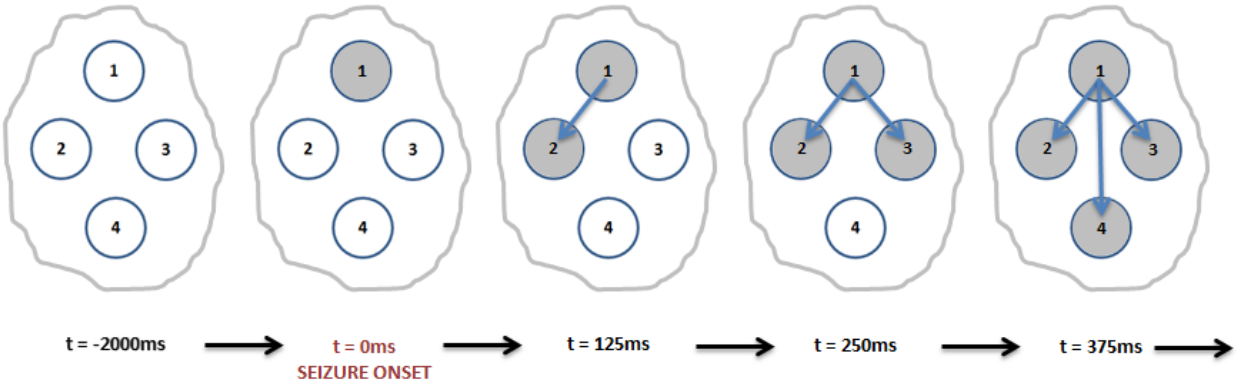

Figure 8.4.1: Four Electrode Simulation Model

The simulation model was expanded to sixteen channels to better model the complexity of neural system and recording electrodes present in the clinical data. The sixteen channels were randomized. Four channels contained the same propagation sequence of the simulated seizure shown in Figure 4.4.1. The remaining twelve channels contained uncorrelated white noise. The short-time and adaptive *swDTF* were once again computed and compared. All results are presented in section 5 of this paper.

4.5 Applying to ECoG recordings

All ECoG data was obtained with permission from Spectrum Health's Epilepsy Monitoring Unit (EMU) in Grand Rapids, MI. As described in Section 2.2.3, epilepsy surgery requires a comprehensive pre-surgical program where the patients may be subject to continuous video-ECoG monitoring. The data used in this study come from two patients recorded suffering from focalized epilepsy. The ECoG was recorded at a 1000Hz sampling rate for twenty-four hours a day over a two-week period via 72 intracranial electrodes implanted on the cerebrum. The anatomical locations and grid layout of the electrodes for Patient 2 are included in detail in Appendix A. The data was annotated by an epileptologist.

Over the two week period, Subject 1 experienced a total of five seizures and Subject 2 experienced a total of fifteen seizures. These annotations include the start and stop times of the particular seizure.

A twenty-second segment of data for each seizure was analyzed. Because of the interest in studying the initial propagation of ictal activity, the twenty second segment of data included five seconds prior to onset and fifteen seconds post onset of the epileptic activity. The data was imported into MATLAB from a European Data Format (EDF) file using EEGLAB and the BioSig toolbox. Each EDF file contains two-hours of data. The twenty-second segment of data described above was extracted from the two-hour set of data.

The first 44 (of 72) channels were analyzed. This was done for three primary reasons: 1) both patients primarily experienced epileptic activity in the temporal region and the frontal regions. These regions did not require analysis above channel 44. 2) A faulty recording device used for channels 63J-72K introduced large amounts of noise into the signal and 3) to save computational time. The twenty-second segment of data was decimated by a factor of four in sampling rate from 1000Hz down to 250Hz. The 250Hz decimated frequency sampling rate proved to accurately represent the dominant frequencies contained in the signal sampled at 1000Hz while minimizing noise (this helps when fitting the MVAR model) and saving computational time. The decimated twenty-second segment of data was used to generate the time-variant MVAR coefficients.

5. Results

5.1 Simulation

A set of simulated signals was generated according to the model described in Figure 4.4.1. A sinusoid with frequency varying from 12Hz (at t=0s) down to 8Hz (at t=3s) generated at a sampling rate of 250Hz was used to simulate a non-stationary seizure. A layer of noise with 5dB signal-to-noise ratio (SNR) was added to the signal to more accurately represent a typical EEG signal. The signals are a total of five seconds in length with two seconds prior to simulated seizure onset and three seconds following simulated seizure onset. The resulting simulated signals are shown below in Figure 5.1.1. The seizure starts at time 0s in channel one and propagates according to Figure 4.4.1.

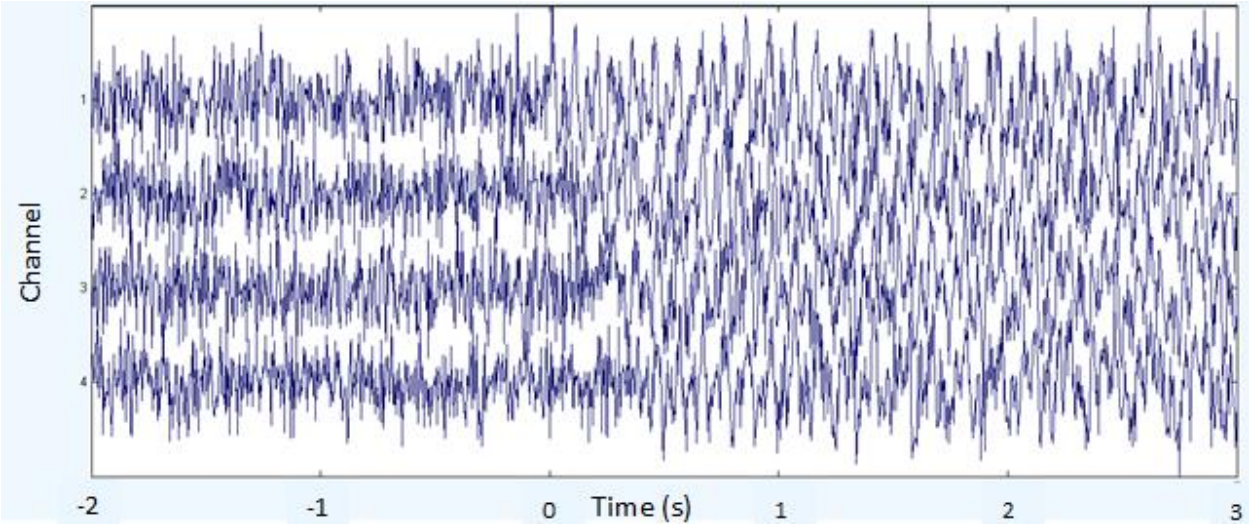

Figure 9.1.1: Simulated Signals with 5dB SNR

Both the *ffADTF* (Eq. 7) and *swADTF* (Eq. 8) were calculated for the simulated signals shown above. A reference output was also calculated. The results are shown below in Figure 5.1.2.

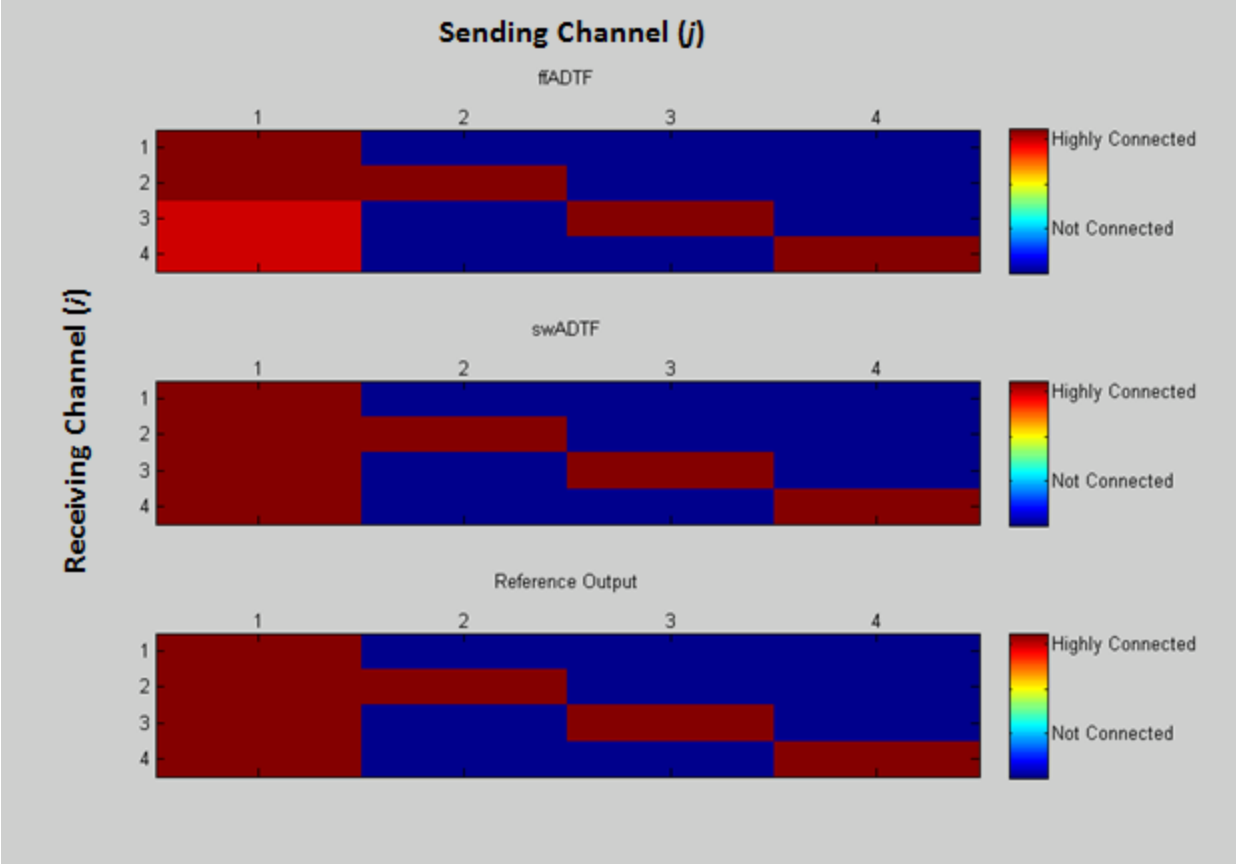

Figure 10.1.2: Simulated Signals Connectivity Results

As can be seen from the figure above, both the *ffADTF* and *swADTF* have results similar to the desired output. Both measures show high connectivity from channel 1 to all other channels in the model. All diagonal plots show high connectivity because the amount of information moving from one signal to itself is obviously very high. The *swADTF* matches the reference output exactly whereas the *ffADTF* shows slightly lower connectivity from channel 1 to channels 3 and 4. The "connectivity image" of Figure 5.1.2 can also be displayed as a simple histogram showing the total reinforcements of a connection from a particular channel to all other channels. The histogram results are shown below in Figure 5.1.3.

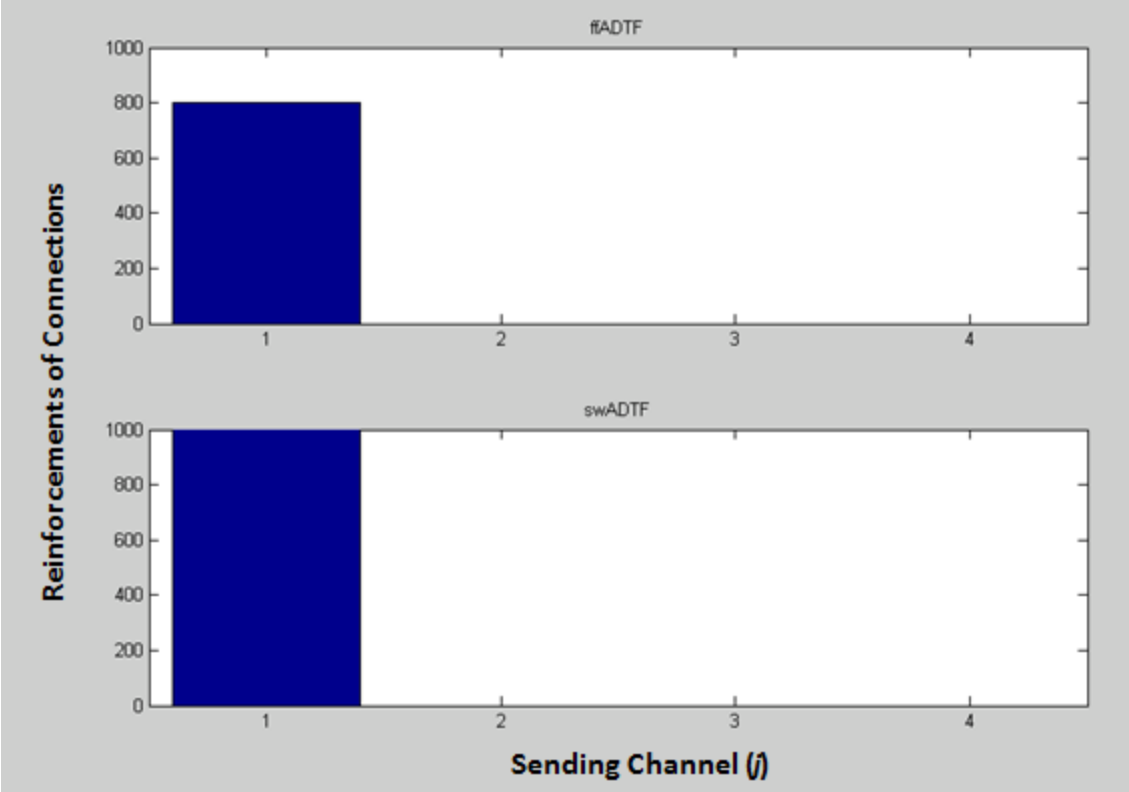

Figure 11.1.3: Simulated Signals Connectivity Histogram

As in Figure 5.1.2, Figure 5.1.3 shows all connections correctly being initiated by channel 1 for both the *ffADTF* and the *swADTF*. In this example, the simulation signals are a total of 5 seconds in length sampled at 250Hz. There are a total of 1250 samples for each signal. The overall reinforcements of a connection are greater for the *swADTF* (1000/1250) compared to the *ffADTF* (800/1250).

The sensitivity (Eq. 9) and specificity (Eq. 10) were calculated for the *ffADTF* and the *swADTF* by comparing the respective output to the reference output. The results are shown in Table 5.1.1.

Table 12.1.1: Sensitivity and Specificity

	ffADTF	swADTF
Sensitivity	**0.8634**	**0.9278**
Specificity	**0.9991**	**0.9993**

Both measures have extremely high specificity and the difference between the two is negligible. The *swADTF* proves superior in sensitivity compared to the *ffADTF* measure. This mostly has to do with the addition of weighing all outgoing information in the transfer function by the autospectrum of the sending (j) signal. This prevents $H_{ij}(f,t)$ from being elevated even when there is no power in the spectrum of that signal at that frequency and time. The *swADTF* was chosen over the *ffADTF* due to this higher sensitivity.

The simulation model was expanded to sixteen channels. The sequence of events in the sixteen channel simulation is the same as in Figure 4.4.1 with the addition of twelve channels containing uncorrelated white noise with 5dB SNR. The propagation sequence of the simulated seizure was randomized and begins in channel 16 before spreading according to Figure 4.4.1 to channels 13, 3, and 4. The *swADTF* results are shown below in Figure 5.1.4.

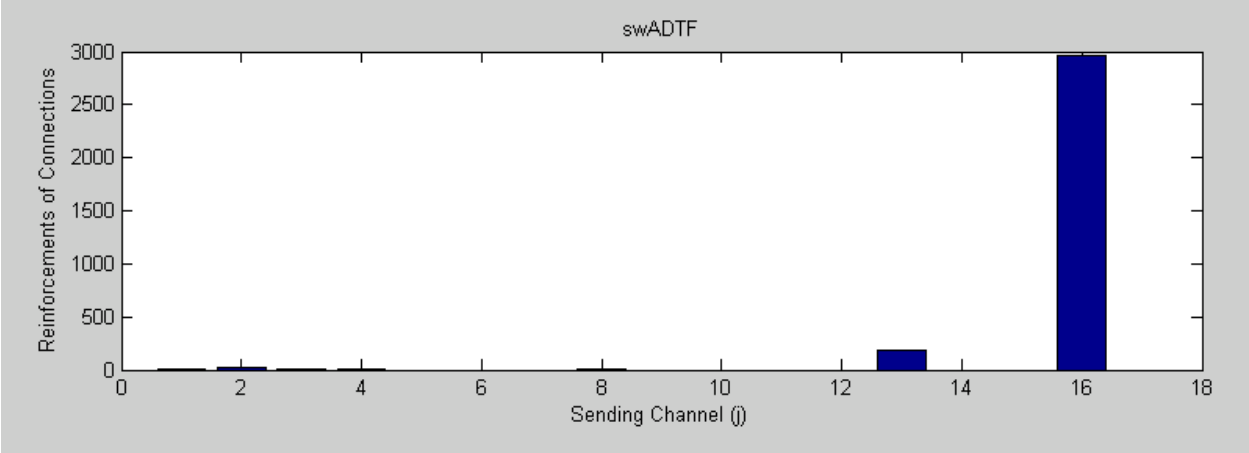

Figure 13.1.4: Expanded Simulated Signals Connectivity Histogram

The *swADTF* measure is successfully able to identify channel 16 as the initiating channel in this expanded simulation.

The short-time *swDTF* was computed for the expanded sixteen channel simulated using a 100ms Hamming window with 50% overlap. The short-time results were compared to the adaptive results. In this instance, the simulated seizure begins in channel 10 before spreading according to Figure 4.4.1 to channels 6, 12, and 2. The results are below in Figure 5.1.5.

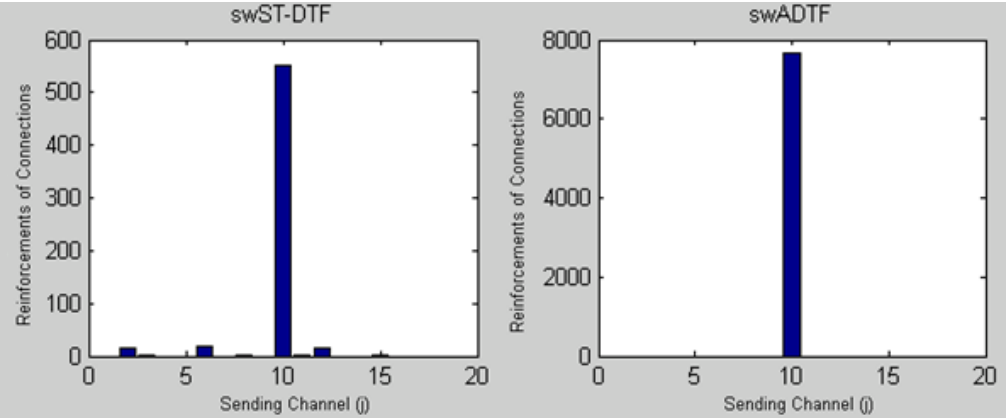

Figure 14.1.5: Short-Time versus Adaptive Simulation Model Results

Both the short-time *swDTF* (swST-DTF) and the adaptive *swDTF* (swADTF) correctly show channel 10 as being the initiating channel for the simulated seizure. Note the large difference in the reinforcements of connections from each plot. The short-time approach has a maximum of around 550 "reinforcements of connections" whereas the adaptive approach has nearly 8000. This difference is mostly due to the large difference in the number of samples. The adaptive approach has a time-variant *swDTF* value at every time point in the signal whereas the short-time approach only has a time-variant *swDTF* value every 50ms. It is also clear that that the short-time approach shows influences from other channels that are not the initiating channel whereas the adaptive approach does not.

In order to better visualize the data, the raw values of the *swDTF* over time can be plotted for each pair of channels. The *swDTF* values between the four channels of the simple simulation over time for both the adaptive and short-time approach are plotted in Figures 5.1.6 and 5.1.7. The green line in each plot shows the uniform threshold used to determine significant connections for the particular measure as shown in previous figures. The red vertical line shows the onset time of the simulated seizure.

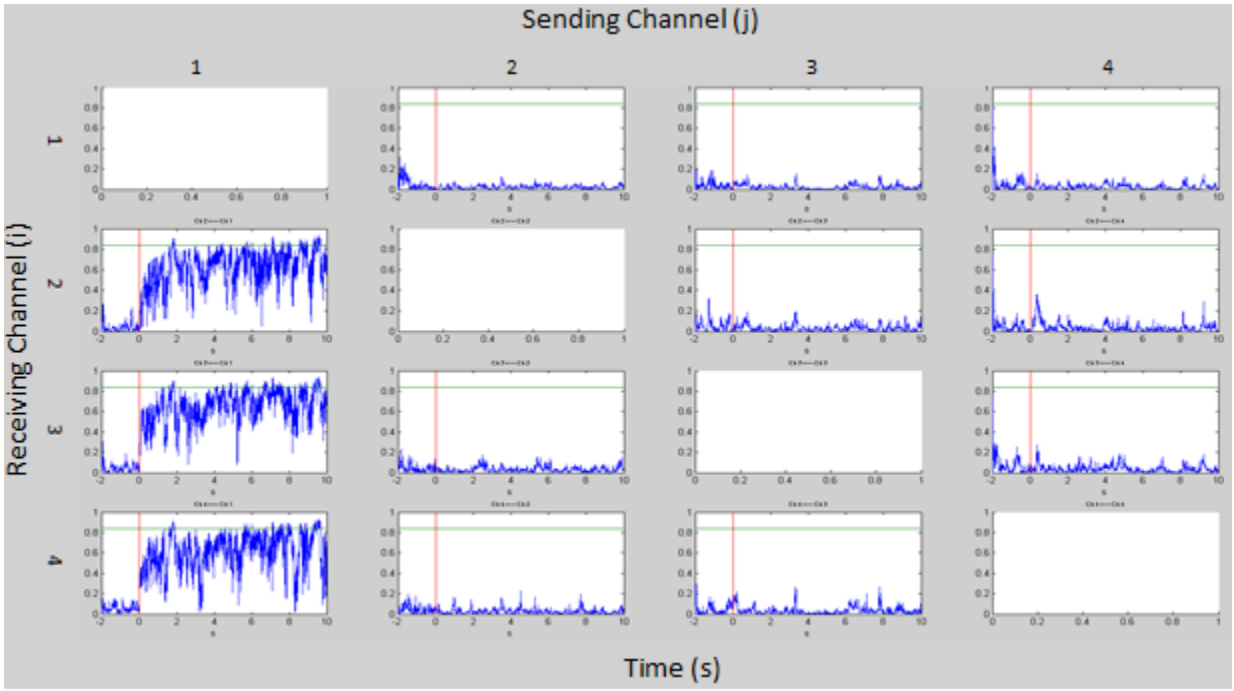

Figure 15.1.6: Raw Adaptive swDTF Values

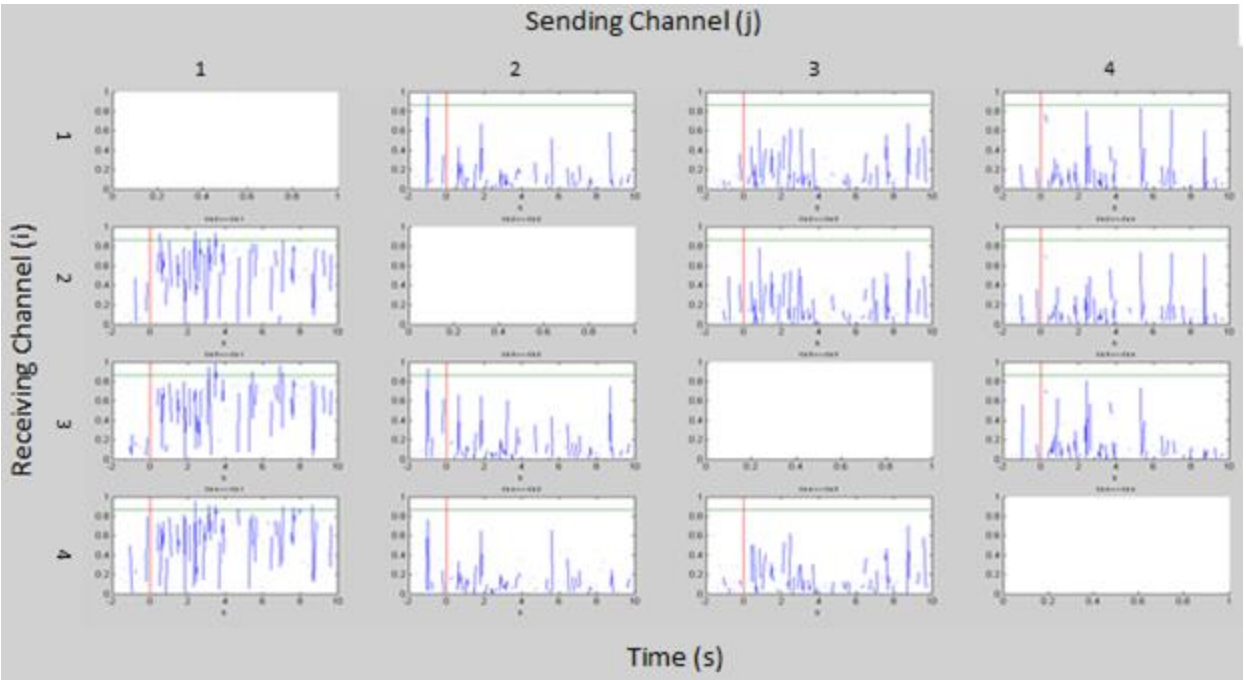

Figure 16.1.7: Raw Short-Time swDTF Values

Both figures show a large increase in the *swDTF* values following onset of the simulated seizure at time t=0s from channel 1 (column 1). The adaptive measure has a slight delay following onset due to the inherent delay in the Kalman filtering algorithm. The short-time approach does not show this delay and immediately reaches threshold following onset of the simulated seizure. On the other hand, the adaptive approach shows much less variation in *swDTF* values in the channels that are not the site of onset (columns 2, 3, and 4).

5.2 Clinical ECoG Data

The short-time and adaptive *swDTF* measures were applied to twenty second segments of the 44 channels for each noted seizure of two different patients during the two week IVEM procedure. Patient 1 experience five seizures and Patient 2 experienced fifteen seizures. Results for all seizures of both patients are included in Appendix B. The anatomical location of each electrode number mentioned throughout this thesis can be found in Appendix A. This section contains two seizures from Patient 2 and one seizure from Patient 1. The results

from Patient 2, seizure 3 are below for the adaptive (Figure 5.2.1) and the short-time (Figure 5.2.2) approaches. The epileptologist noted channels 27-42D and specifically channels 34C, 39D, 40D, and 41D as electrodes of interest for the particular seizure.

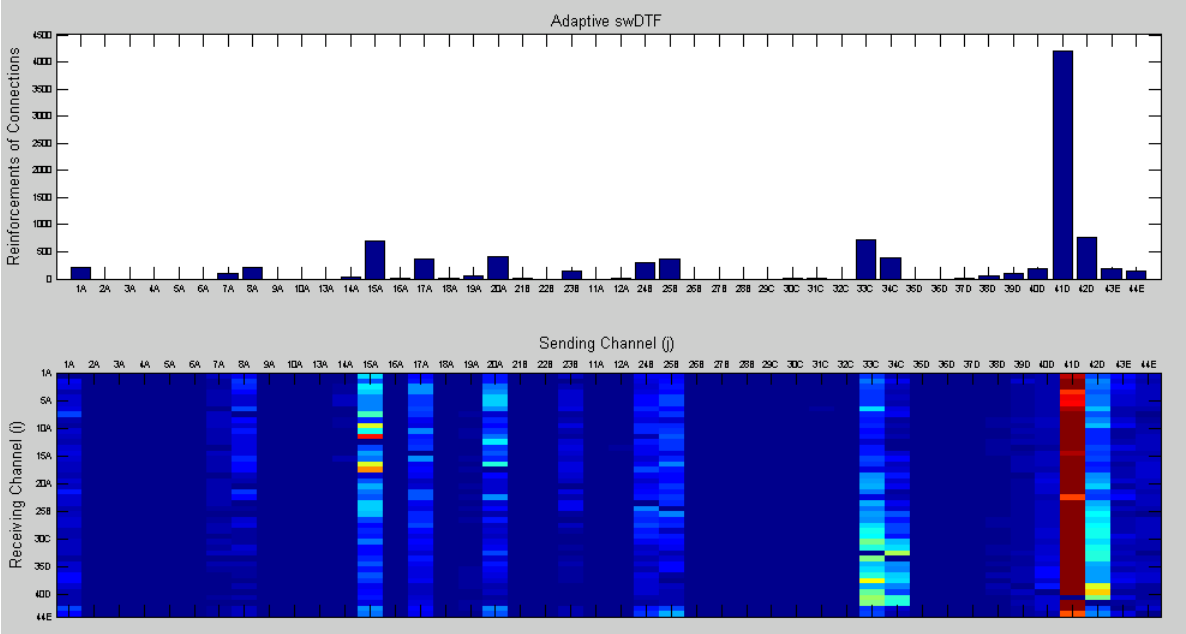

Figure 17.2.1: Adaptive swDTF for Patient 2, Seizure 3

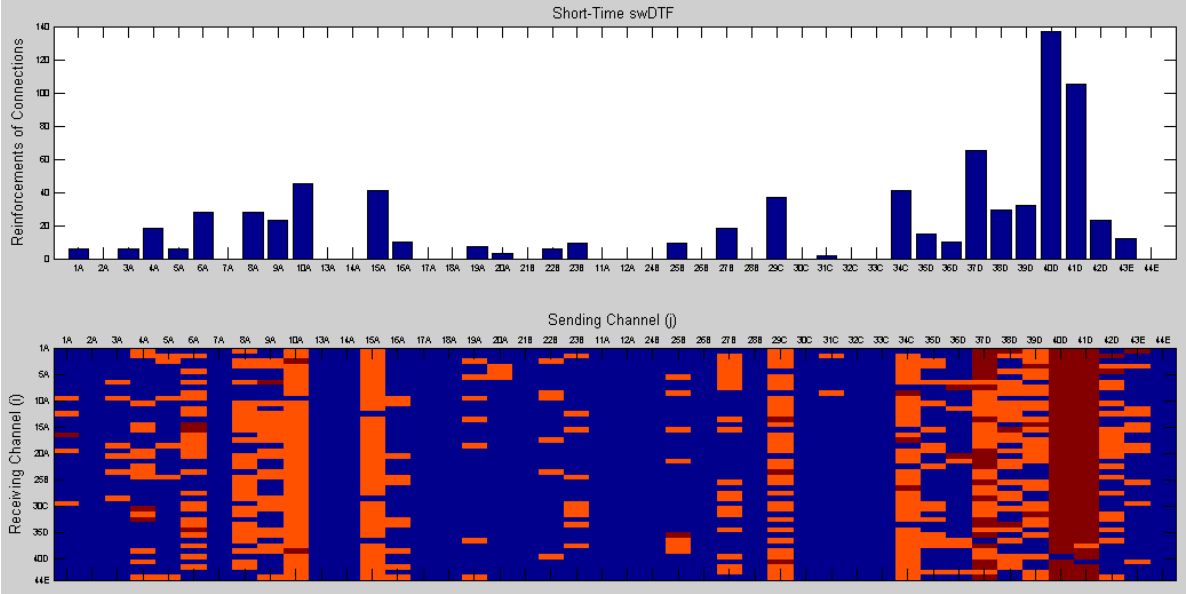

Figure 18.2.2: Short-Time swDTF for Patient 2, Seizure 3

Both measures successfully identify the correct region of interest as denoted by the epileptologist. The adaptive measure pinpoints channel 41 as the epileptogenic focus whereas the short-time measure shows elevated levels of connectivity for channels 34C-42D and specifically channels 40D and 41D. These results are consistent with simulations with the short-time approach tending to show more influence from additional channels than the adaptive approach. The bottom plot shows the interaction between each pair of channels. It is clear that the adaptive measure provides a more meaningful plot of this interaction between pairs channels than the short-time measure mostly due to the number of samples each measure is estimated with.

For Patient 2, seizure 1, the epileptologist noted channels 34C-42D and specifically channels 34C, 40D, 41D, and 42D as electrodes of interest for the particular seizure. The results are below in Figures 5.2.3 and 5.2.4.

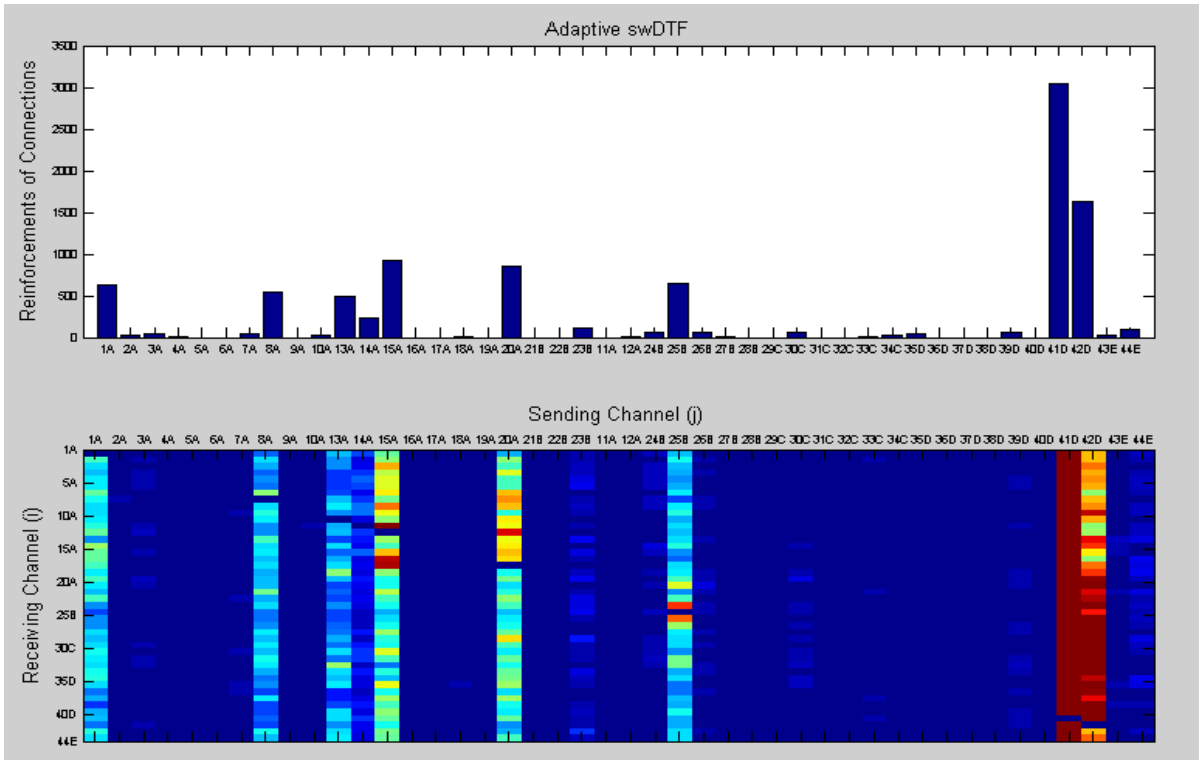

Figure 19.2.3: Adaptive swDTF for Patient 2, Seizure 1

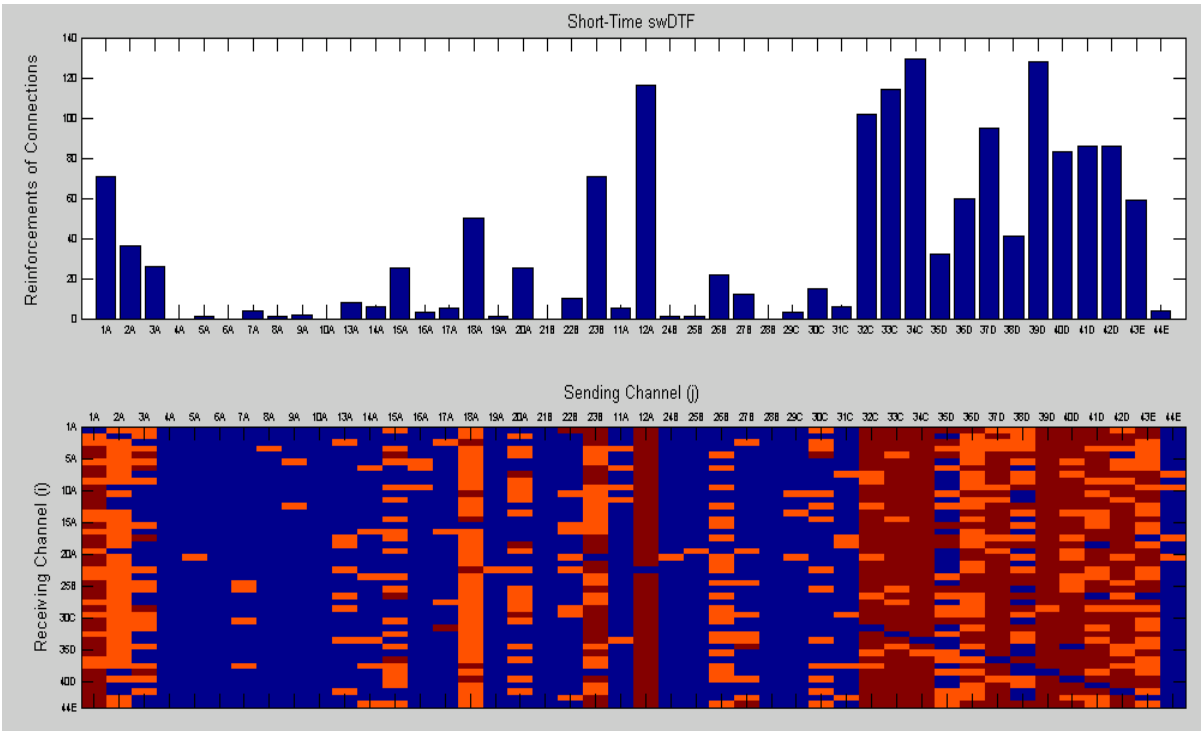

Figure 20.2.4: Short-Time swDTF for Patient 2, Seizure 1

Once again, both measures successfully identify the general region of interest as noted by the epileptologist. The short-time approach is spread out over many channels from 32C-43E whereas the adaptive approach only identifies channels 41D and 42D. The short-time approach also shows high connectivity values for channels not noted by the epileptologist (1A, 23B, 12A).

For Patient 1, seizure 1, the epileptologist noted channels 51-55J, 26D as electrodes of interest for the particular seizure. Channels 17C-59K were analyzed for this patient. The results are below in Figures 5.2.5 and 5.2.6.

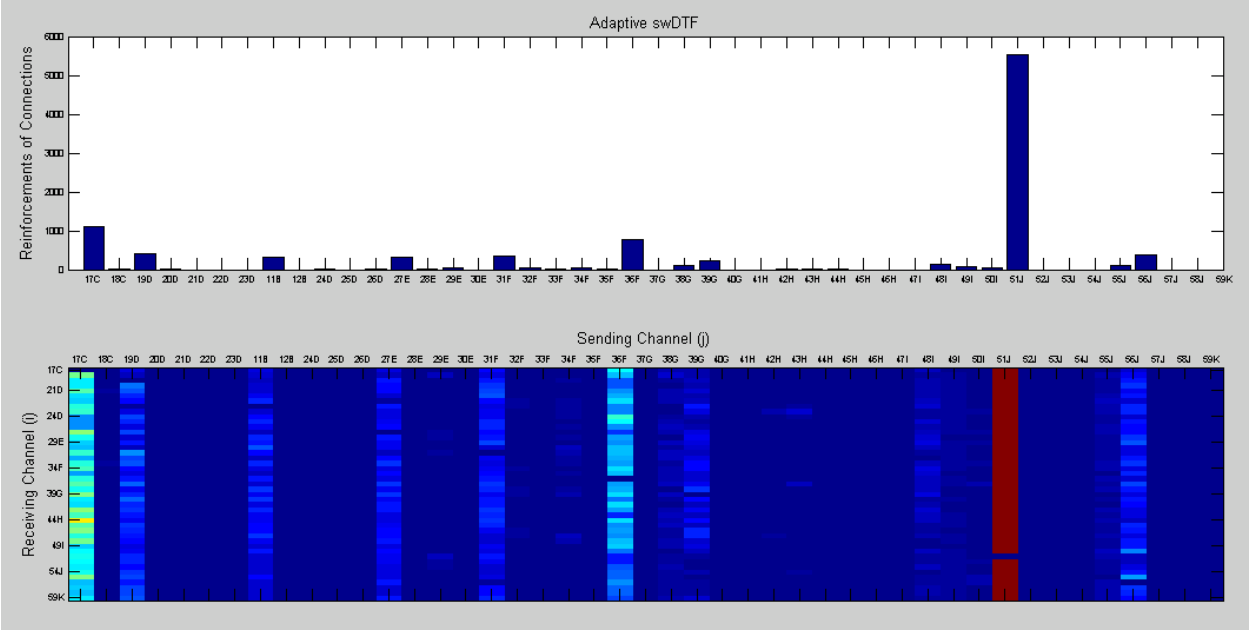

Figure 21.2.5: Adaptive swDTF for Patient 1, Seizure 1

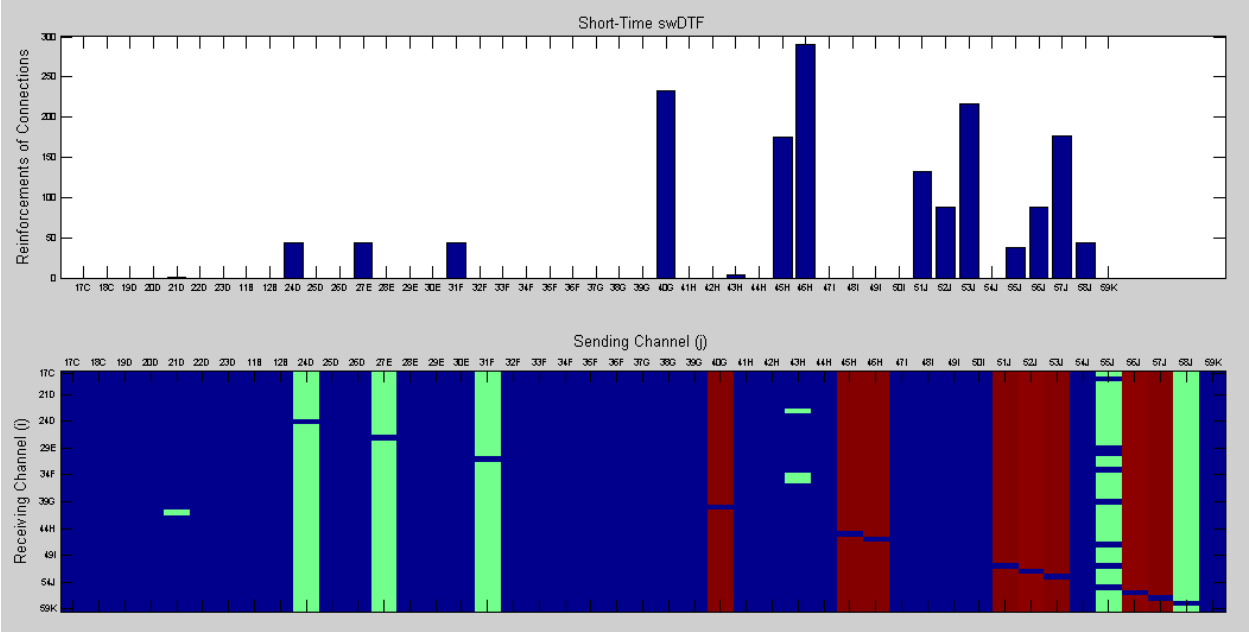

Figure 22.2.6: Short-Time swDTF for Patient 1, Seizure 1

In this case, the adaptive approach successfully identifies an electrode within the region noted by the epileptologist (electrode 51J). The adaptive approach also shows slightly elevated connectivity values for channel 36F. This channel was noted by the epileptologist. Channel 17C shows slightly elevated connectivity and was not noted by the expert. The short-time approach shows elevated connectivity values from 51-57J. This is consistent with the expert observations. The highest connectivity values, however, are noted in channels 40G and 46H which were not channels noted by the expert. The remaining results are included in Appendix B.

Both the time-variant *swDTF* and *ffDTF* measures were successful at identifying the simulated epileptogenic focus in the simple and expanded simulations. The *swDTF* proved to have higher sensitivity than the *ffDTF* and was chosen over the *ffDTF* for use with clinical data. Both the short-time and adaptive approaches were able to identify electrodes of interest

consistent with findings from the expert epileptologist. The adaptive approach, however, was much better at pinpointing an exact electrode whereas the short-time approach showed elevated connectivity levels for a large region of electrodes.

6. Discussion

The simulation model generated was able to verify that the time-variant *swDTF* was successful at analyzing a spreading, non-stationary signal and determining the source of that signal. The simulation confirmed that both the adaptive *ffDTF* and *swDTF* were able to identify the simulated epileptogenic focus (Figure 5.1.2 and 5.1.3). Both measures had very high specificity (0.999) and a sensitivity of at least 86%. The *swDTF* had higher sensitivity (93%) than the *ffDTF* (86%). This is mostly due to the additional weighting by the autospectra of the sending signal in the *swDTF* measure.

After moving forward with the *swDTF*, the measure continued to prove itself after successfully identifying the simulated epileptogenic focus in more advanced simulations (Figure 5.1.4). The adaptive *swDTF* was then compared to a much simpler short-time *swDTF* using the same expanded sixteen channel simulation model. Both measures proved successful at identifying the simulated epileptogenic focus. The short-time approach showed more additional channels with elevated connectivity than did the adaptive approach (Figure 5.1.5). This is mostly due to the vast difference in the number of samples used in the two methods. The adaptive approach is modeled for every time point (i.e., 250 samples per second) in the data whereas the short-time approach is only modeled one time within each window (i.e., 20 samples per second). The result is a total of 5000 samples for the adaptive *swDTF* compared to only 400 for the short-time *swDTF*. This observation was consistent throughout analysis of all simulated and physiological data. This difference was also confirmed when observing the raw *swDTF* values (Figures 5.1.6 and 5.1.7). The adaptive measure exhibited much less fluctuation in the *swDTF* values and shows values consistently below the threshold in sending channels that are not the epileptogenic focus. The short-time measure expresses a much more sporadic pattern

with values coming very close to or even exceeding the threshold in sending channels that are not the epileptogenic focus.

The results from applying the short-time and adaptive measures to twenty second ictal segments of ECoG data were promising. Both measures showed elevated connectivity levels sent from channels of interest noted by the epileptologist. The adaptive measure was typically able to pinpoint one or two channels of interest whereas the short-time measure identified a larger region. This is evident in Figures 5.2.3 and 5.2.4. The electrodes of interest were identified by the expert to be from 37-42D. The adaptive approach identified channels 41 and 42D whereas the short-time approach identified the region from 32C-43E. Again, this discrepancy can mostly be explained by the large difference in the number of samples used for each measure. The lesser number of samples that the short-time approach is calculated with makes the measure more susceptible to noise in the signal. The short-time approach also requires the assumption of a stationary signal within the 100ms window. This may not be the case during onset of an epileptic seizure. The adaptive approach can be used to more accurately model this highly non-stationary behavior. The short-time approach also proved to be extremely sensitive to parameter changes in the measure. Window size, percent overlap, MVAR model order, MVAR estimation mode (e.g., Nutall-Strand versus Vieira-Morf) all greatly affected the outcome of the measure. The adaptive measure proved more robust. All of these factors played a role in both increasing the short-time *swDTF* values for channels not involved in the propagation of the seizure and introducing variation between the two methods.

The largest benefit of the short-time approach was a drastic reduction in computation time. Whereas the adaptive approach takes approximately 12 hours to analyze a single seizure, the short-time approach took only 30 minutes (running on Intel Xeon CPU E5-2637 with 64GB of

RAM). The short-time approach is also much less computationally intensive than the adaptive approach and can therefore be used on more common machines.

Overall, the adaptive approach was able to successfully identify the electrodes of interest (± 10mm) as noted by the epileptologist as the electrode with the largest reinforcements of connections (largest histogram value) in 14 out of 16 (88%) seizures for the two patients. The short-time approach was able to identify a region of 30-100mm within the region of interest as noted by the epileptologist in 12 out of 16 (75%) seizures for the two patients.

7. Future Work

In the future, it is important to verify the results of the various time-variant *swDTF* measures. Up until now, the only verification performed has been on simulated data by calculating the sensitivity and specificity of the measures. When applying to ECoG data, the current available methods for verifying results simply involve comparing electrodes with high *swDTF* values with electrodes of interest noted by the epileptologist. Actual verification of the *swDTF* results with the resected tissue would be possible with post-operational magnetic resonance imaging (MRI). These post-operational images are not currently available for the subjects studied in this work due to the long follow-up time currently required by the EMU.

The short-time version of the *swDTF* measure can be refined in a number of ways. All parameters (window size, percent overlap, model order, model estimation mode, etc.) were empirically determined. Verification other than using a simple simulation is recommended and the parameters may be optimized with more experimentation.

The recent availability of ECoG data from approximately ten additional patients leaves testing the measure on the additional patients an option. This would provide results that can help with refining the measure and realizing the robustness of the measure on a large number of patients.

Finally, the ability of the measure to function as a simple plugin to the open-source EEGLAB software is ideal. The measure is currently run as a MATLAB function. Creating an EEGLAB plugin would allow easy access and customization to the measure along with the other tools already included in the EEGLAB package.

8. Conclusion

This thesis contributes to the area of epilepsy surgery by introducing a quantitative measure that may help both aid the surgeon in delineating a potential epileptogenic focus and reduce the overall procedure time. The measure is known as the time-variant spectrum – weighted directed transfer function (*swDTF*) and was able to correctly identify the epileptogenic focus in a simulation model with sensitivity of 0.93 and specificity of 0.99. When applied to clinical data, the adaptive version of the *swDTF* successfully identified the electrode of interest (± 10mm) as noted by the epileptologist in 88% of seizures analyzed. The short-time version of the *swDTF* successfully identified a region of 3-10 electrodes (30-100 mm) in 75% of seizures analyzed. The methods and findings of this thesis are concluded in detail below.

The ability of a time-variant directed transfer function measure known as the spectrum-weighted directed transfer function to identify elevated information transfer from a particular electrode as the possible epileptogenic region was studied. Two different methods using multivariate autoregressive models were used to generate the time-variant measures. One method used an adaptive Kalman filtering approach and another method used a short-time approach. The two methods were compared using a simulation model and clinical ECoG data.

The simulation of neural connections revealed the superiority of the time-variant swDTF over the ffDTF. Both measures had high specificity (0.999) but the sensitivity of the swDTF (0.93 over 0.86) led to it being chosen over the ffDTF for use with clinical data. When applied to ECoG data, both the adaptive and short-time approach were able to successfully identify electrodes within the region of interest. The adaptive approach was able to

successfully identify the electrodes of interest (± 10mm) as noted by the epileptologist as the electrode with the largest reinforcements of connections (largest histogram value) in 14 out of 16 (88%) seizures for the two patients. The short-time approach was able to identify a region of 30-100mm within the region of interest as noted by the epileptologist in 12 out of 16 (75%) seizures for the two patients. Although the short-time approach had the major benefit of greatly reducing computation time, the adaptive approach is currently preferred mostly due to its robustness in terms of changes to input parameters. The adaptive approach is also better able to pinpoint the exact electrode (±10mm) whereas the short-time approach is better at identifying a general region of interest (30-100mm). Another reason for choosing the adaptive approach is because of the short-time's need for stationarity within the window. It is suggested that the short-time approach be used to gain quick insight into the general region of interest for the seizure and to later pinpoint the potential epileptogenic tissue using the adaptive measure.

9. Bibliography

1. Mierlo P, Carrette E, Hallez H, et al. Ictal-onset localization through connectivity analysis of intracranial EEG signals in patients with refractory epilepsy. *Epilepsia*. 2013.

2. Sakkalis V. Review of advanced techniques for the estimation of brain connectivity measured with EEG/MEG. *Comput Biol Med*. 2011;41(12):1110-1117.

3. Horwitz B. The elusive concept of brain connectivity. *Neuroimage*. 2003;19(2):466-470.

4. Wilke C, Ding L, He B. Estimation of time-varying connectivity patterns through the use of an adaptive directed transfer function. *Biomedical Engineering, IEEE Transactions on*. 2008;55(11):2557-2564.

5. Omidvarnia A, Mesbah M, O'Toole JM, Colditz P, Boashash B. Analysis of the time-varying cortical neural connectivity in the newborn EEG: A time-frequency approach. . 2011:179-182.

6. Liang H, Ding M, Nakamura R, Bressler SL. Causal influences in primate cerebral cortex during visual pattern discrimination. *Neuroreport*. 2000;11(13):2875-2880.

7. Omidvarnia A, Mesbah M, Khlif M, O'Toole J, Colditz P, Boashash B. Kalman filter-based time-varying cortical connectivity analysis of newborn EEG. . 2011:1423-1426.

8. Arnold M, Milner X, Witte H, Bauer R, Braun C. Adaptive AR modeling of nonstationary time series by means of kalman filtering. *Biomedical Engineering, IEEE Transactions on*. 1998;45(5):553-562.

9. Kaiser DA. Basic principles of quantitative EEG. *Journal of Adult Development*. 2005;12(2-3):99-104.

10. Subha DP, Joseph PK, Acharya R, Lim CM. EEG signal analysis: A survey. *J Med Syst*. 2010;34(2):195-212.

11. About epilepsy. The Epilepsy Foundation Web site. http://www.epilepsyfoundation.org/aboutepilepsy/. Accessed 11/08, 2013.

12. Fisher R. Overview of epilepsy. *Book of Comprehensive Epilepsy Cente*r. 1997.

13. van Mierlo P, Carrette E, Hallez H, et al. Accurate epileptogenic focus localization through time-variant functional connectivity analysis of intracranial electroencephalographic signals. *Neuroimag*e. 2011;56(3):1122-1133.

14. Brodie MJ, Schachter SC, Kwan PKL. *Fast facts: Epilepsy.* Health Press; 2012.

15. Kitagawa G. *Introduction to time series modeling.* 1st ed. Hoboken: Taylor and Francis; 2010:83-105.

16. Granger CW. Investigating causal relations by econometric models and cross-spectral methods. *Econometrica: Journal of the Econometric Societ*y. 1969:424-438.

17. Geweke J. Measurement of linear dependence and feedback between multiple time series. *Journal of the American Statistical Associatio*n. 1982;77(378):304-313.

18. Baccalá LA, Sameshima K. Partial directed coherence: A new concept in neural structure determination. *Biol Cyber*n. 2001;84(6):463-474.

19. Kamiński M, Ding M, Truccolo WA, Bressler SL. Evaluating causal relations in neural systems: Granger causality, directed transfer function and statistical assessment of significance. *Biol Cyber*n. 2001;85(2):145-157.

20. Walter DO. Coherence as a measure of relationship between EEG records. *Electroencephalogr Clin Neurophysio*l. 1968;24(3):282.

21. Thatcher R, North D, Biver C. EEG and intelligence: Relations between EEG coherence, EEG phase delay and power. *Clinical Neurophysiolog*y. 2005;116(9):2129-2141.

22. Wilke C, Ding L, He B. An adaptive directed transfer function approach for detecting dynamic causal interactions. . 2007:4949-4952.

23. Korzeniewska A, Mańczak M, Kamiński M, Blinowska KJ, Kasicki S. Determination of information flow direction among brain structures by a modified directed transfer function (dDTF) method. *J Neurosci Method*s. 2003;125(1):195-207.

24. Schneider T, Neumaier A. Algorithm 808: ARfit—A matlab package for the estimation of parameters and eigenmodes of multivariate autoregressive models. *ACM Transactions on Mathematical Software (TOMS)*. 2001;27(1):58-65.

24. Marple Jr, S. Lawrence. "Digital spectral analysis with applications." *Englewood Cliffs, NJ, Prentice-Hall, Inc., 1987, 512 p.* 1 (1987).

10. Appendix A: Electrode Locations

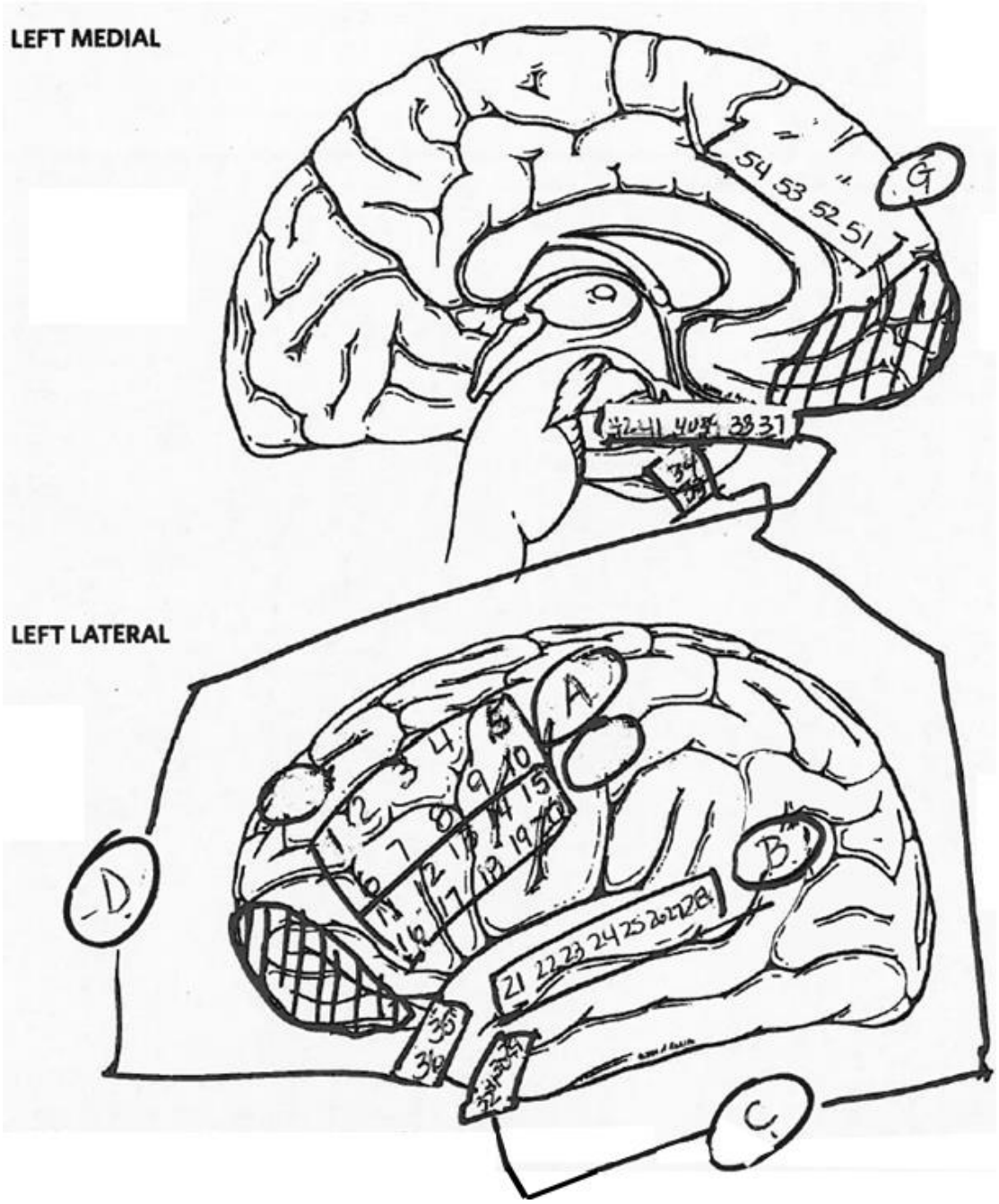

SUBTEMPORAL

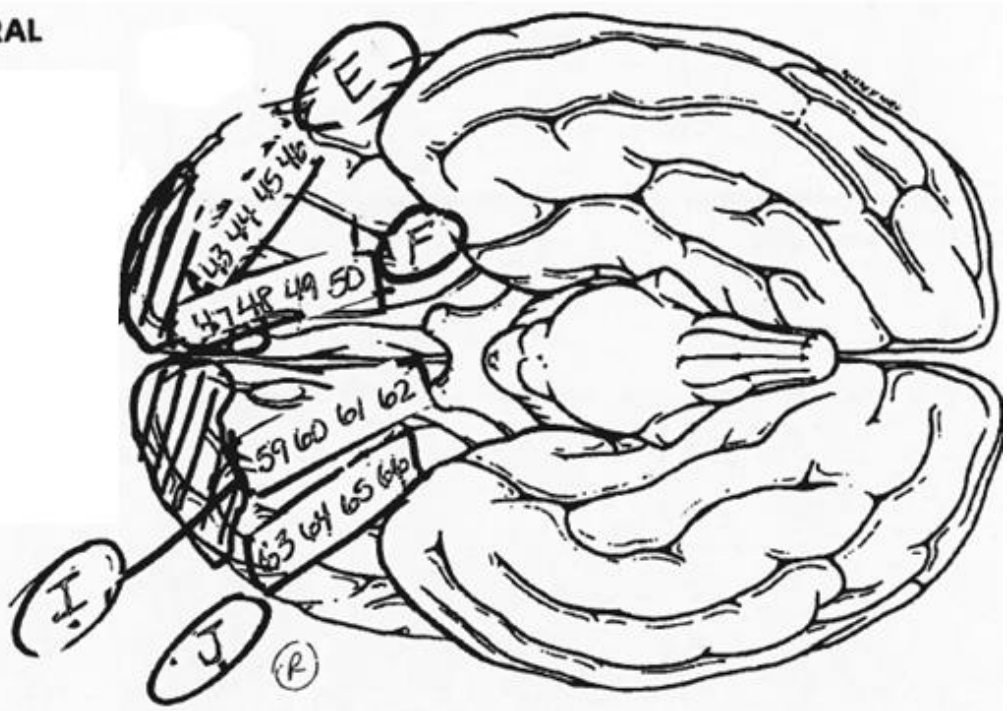

SUPERIOR

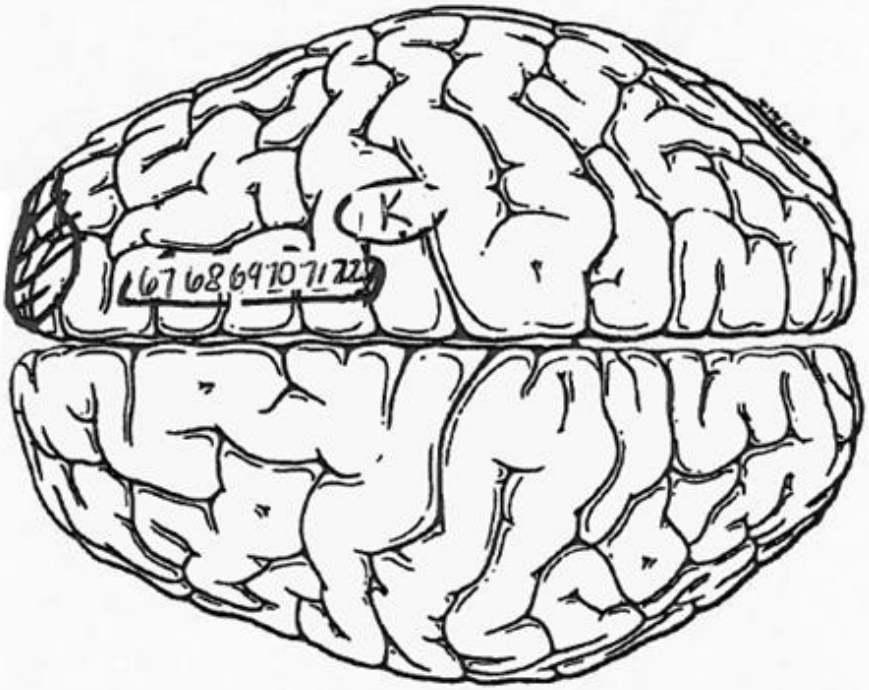

Table A1: Electrode Grids

Grid	Electrode Number
A	1-20
B	21-28
C	29-34
D	35-42
E	43-46
F	47-50
G	51-54
H	55-58
I	59-62
J	63-66
K	67-72

11. Appendix B: Complete Results

Subject 2:

Seizure #1. Repetitive spike-wave discharges (5 to 6 Hz) were noted at electrode contacts D37-42 for 1 second at 21:01:23 on 6/12/2012. This was followed by an electrodecrement/beta buzz at 21:01:25. This evolved into a high-amplitude spike pattern maximum at contacts 39, 40, and 34. This pattern evolved, becoming higher in amplitude and slower in frequency before spontaneously terminating at 21:02:22. Clinically, the patient did not show any significant changes when he was tested by nursing personnel at 21:02:30. He informed the nurse that he was doing okay.

Adaptive Results:

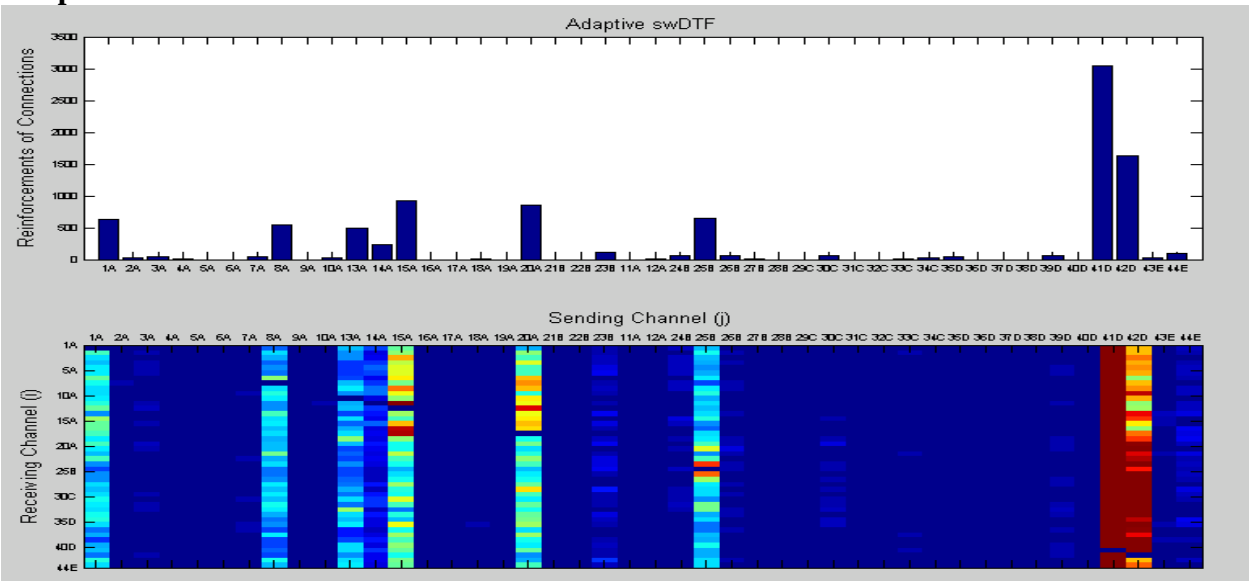

Short-Time Results:

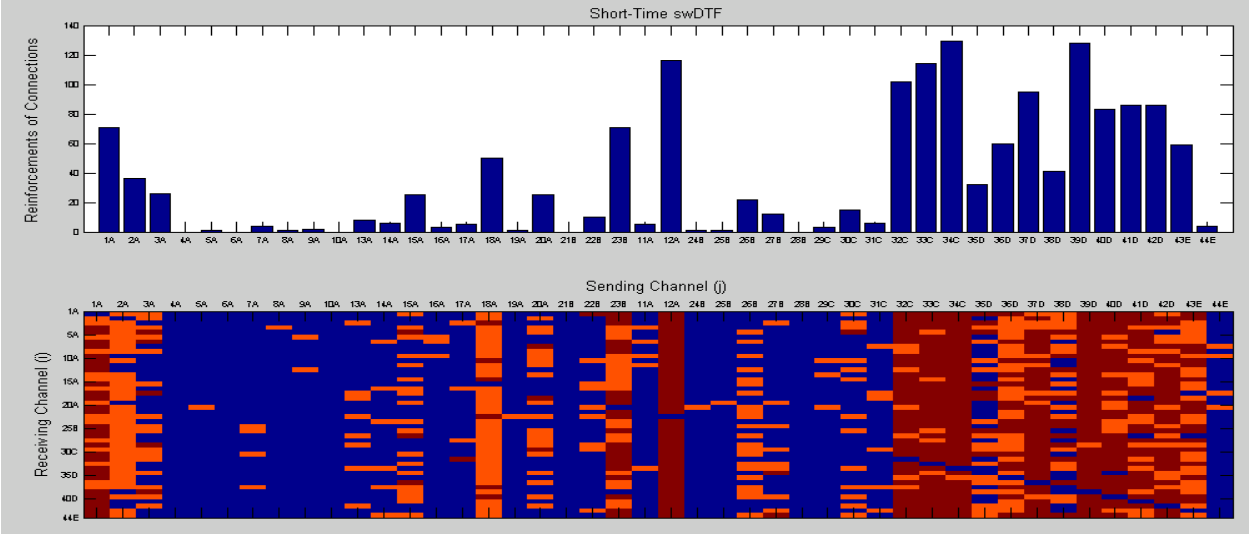

Seizure #2. Electrographically, high-amplitude repetitive spikes were noted at electrodes 40-42 and 34 at 23:47:54. This was followed by an electrodecrement/beta buzz at 23:47:56 and then evolved into a high-amplitude spike and polyspike repetitive pattern (6 to 7 Hz) at 23:47:57. This evolved becoming higher in amplitude and slower in frequency before spontaneously terminating at 23:49:05. Clinically, the patient was not noted to demonstrate any changes nor did he inform nursing of any change in feeling.

Adaptive Results:

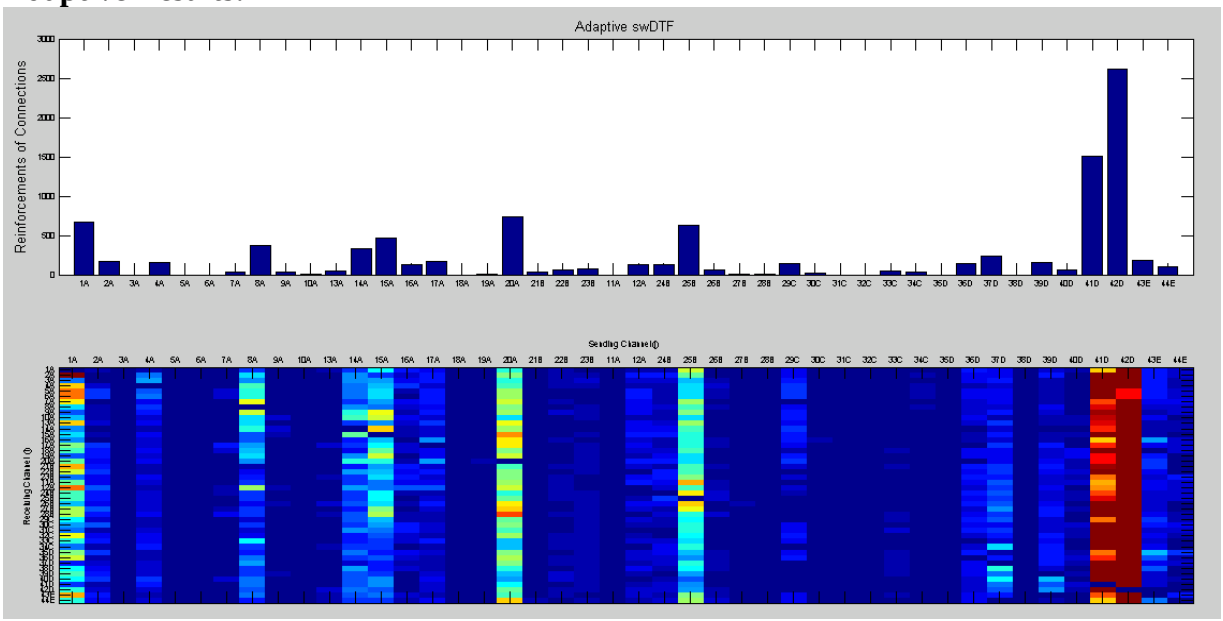

Short-Time Results:

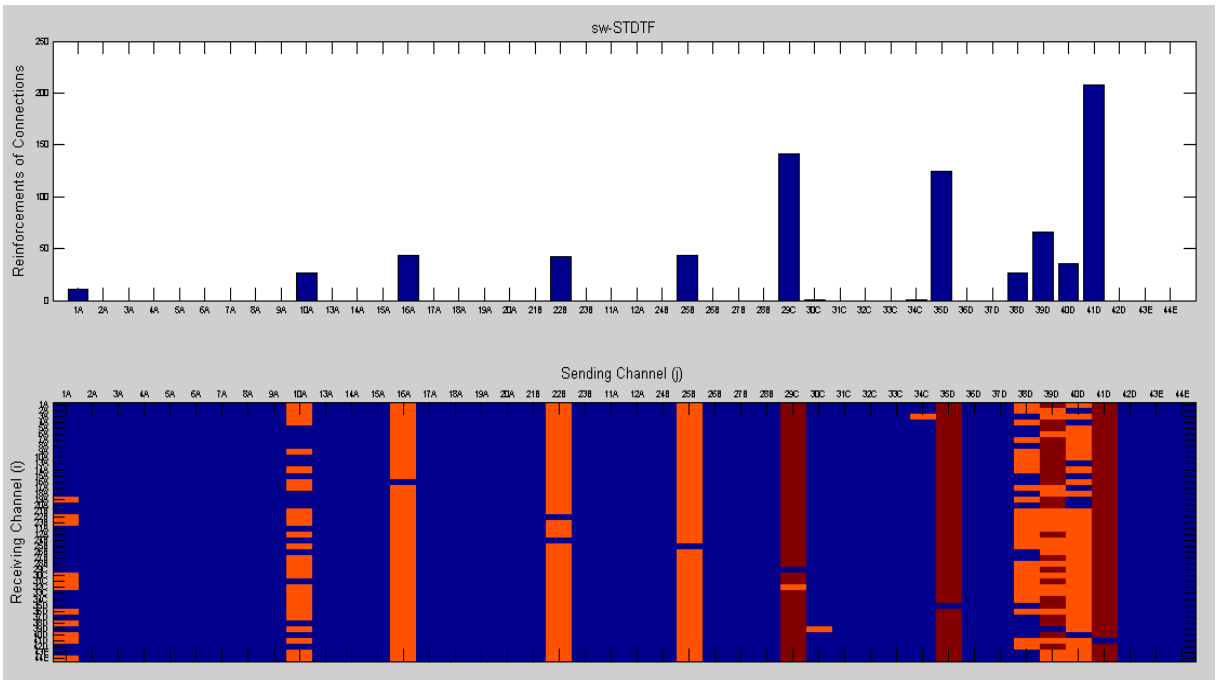

Seizure #3. Electrographically, similar ictal pattern beginning with repetitive spikes was noted at 01:49:27. This evolved with an electrodecrement/beta buzz at 01:49:25 and then evolved into a higher amplitude with repetitive spike-wave discharge. It evolved to a higher amplitude with slower frequency before spontaneously terminating.
No clinical changes were noted.

Adaptive Results:

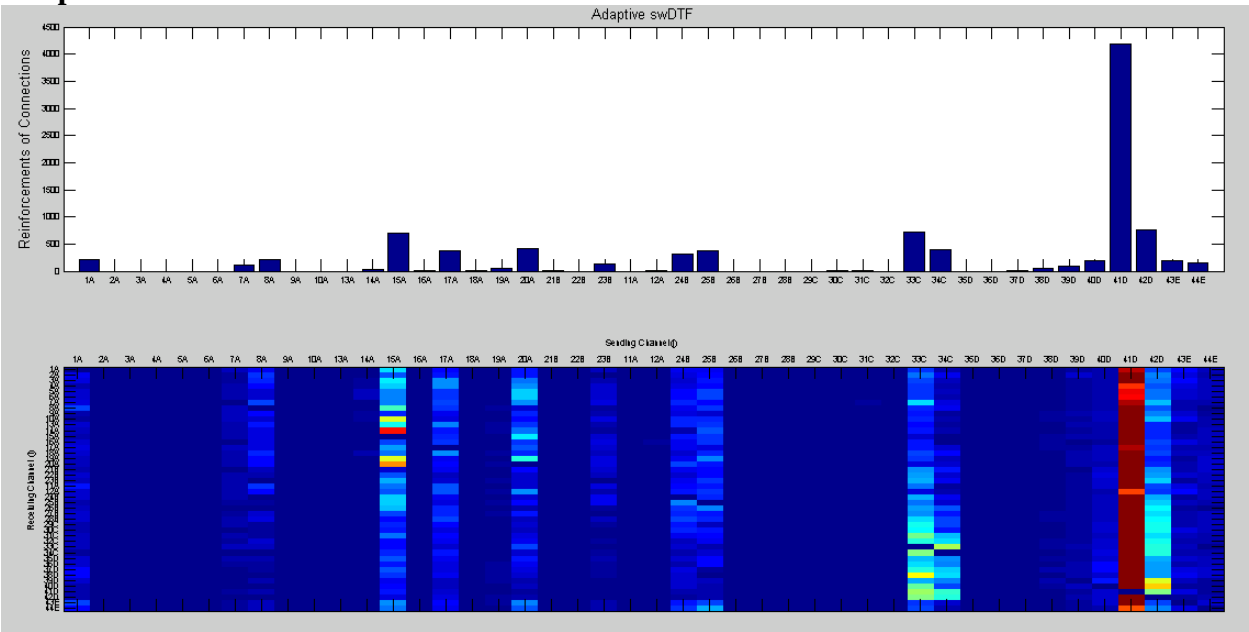

Short-Time Results:

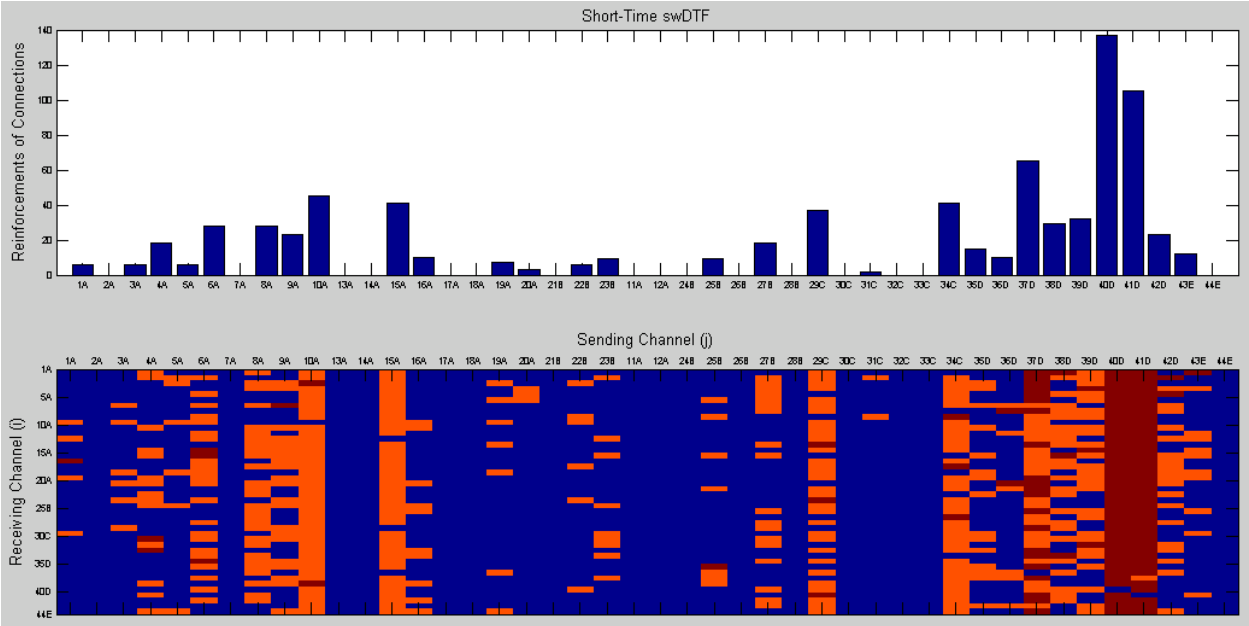

Seizure #4. Electrographically, a repetitive spike pattern was noted over the left mesiotemporal surface at 05:02:21, similar to the 3 previous subclinical electrographic seizures. This, again, evolved over approximately 1 minute before spontaneously terminating.
No definitive clinical changes were noted.

Adaptive Results:

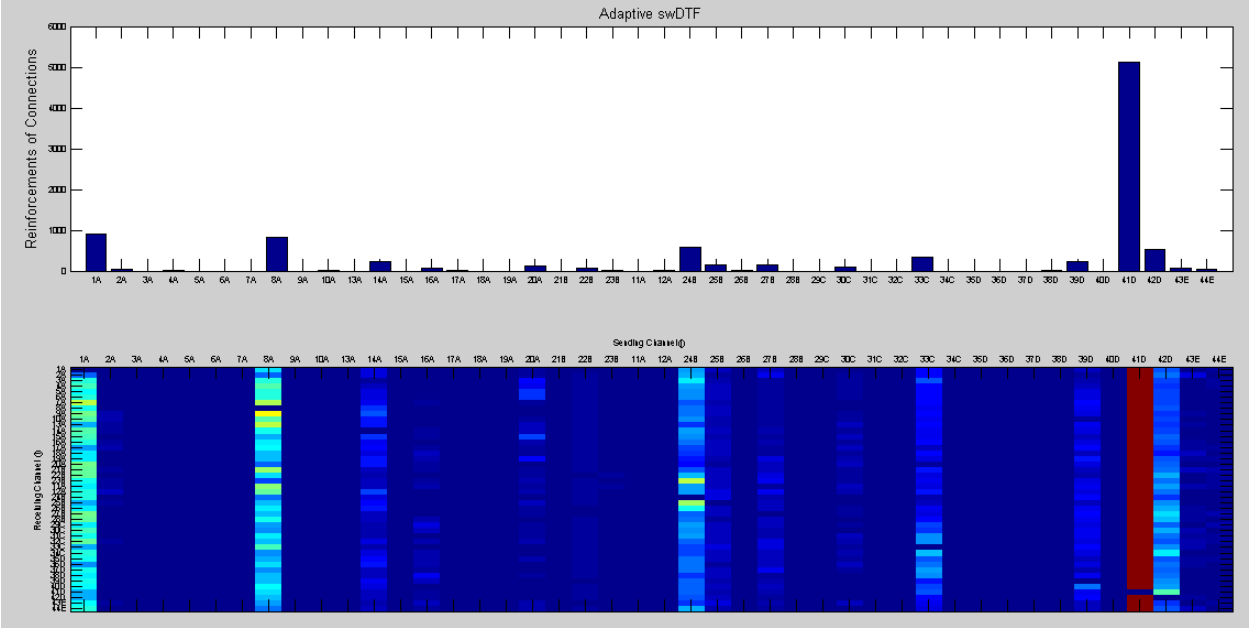

Short-Time Results:

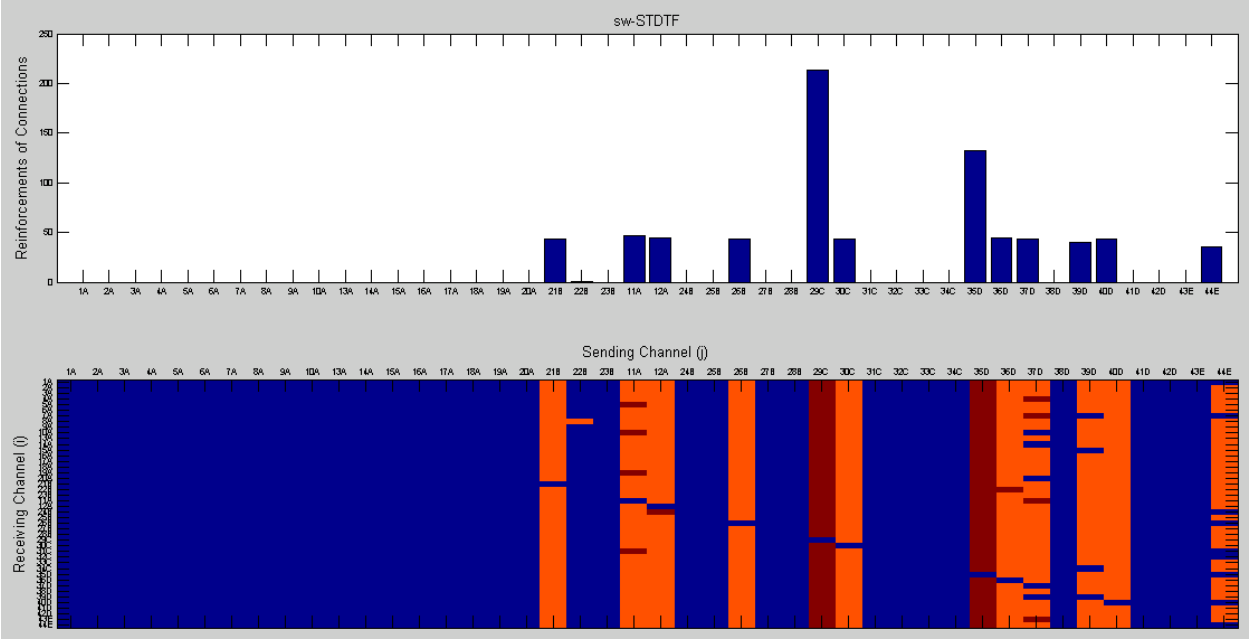

Seizure #5. Electrographically repetitive spikes were noted at 07:33:19 at electrodes 38-42 and electrodes 34 and 45. This was followed by an attenuation/beta buzz at 07:33:20 followed by an ictal evolving pattern becoming higher in amplitude and slower in frequency before terminating at 7:35:35.

Adaptive Results:

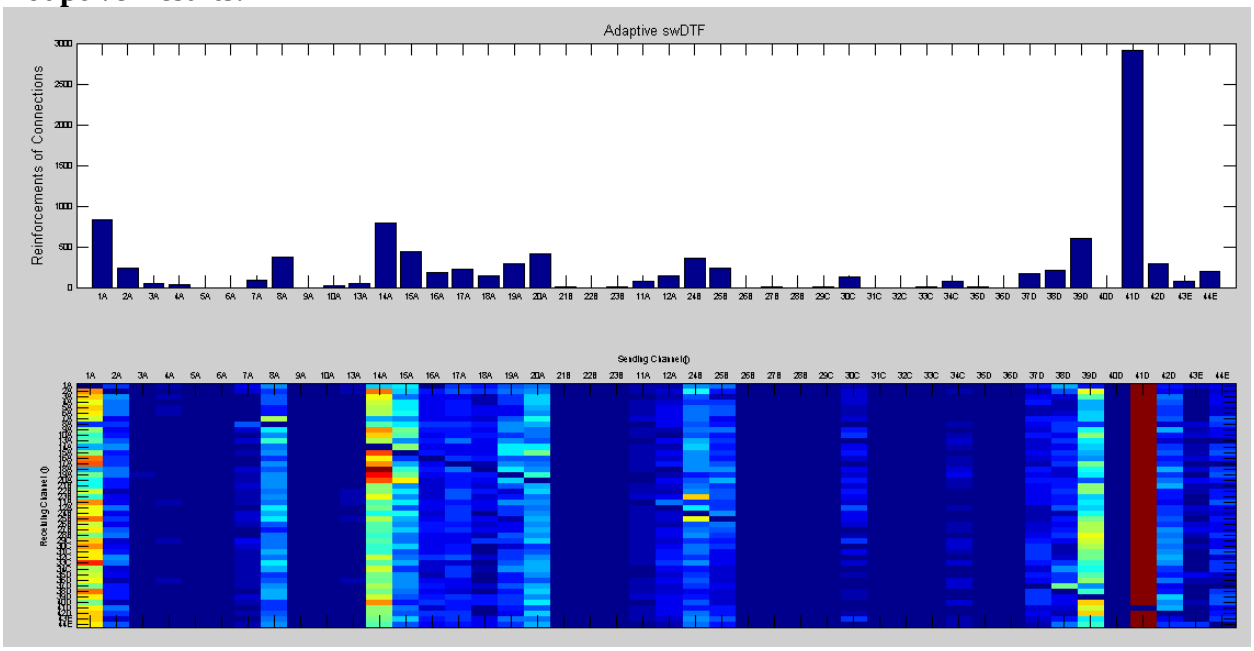

Short-Time Results:

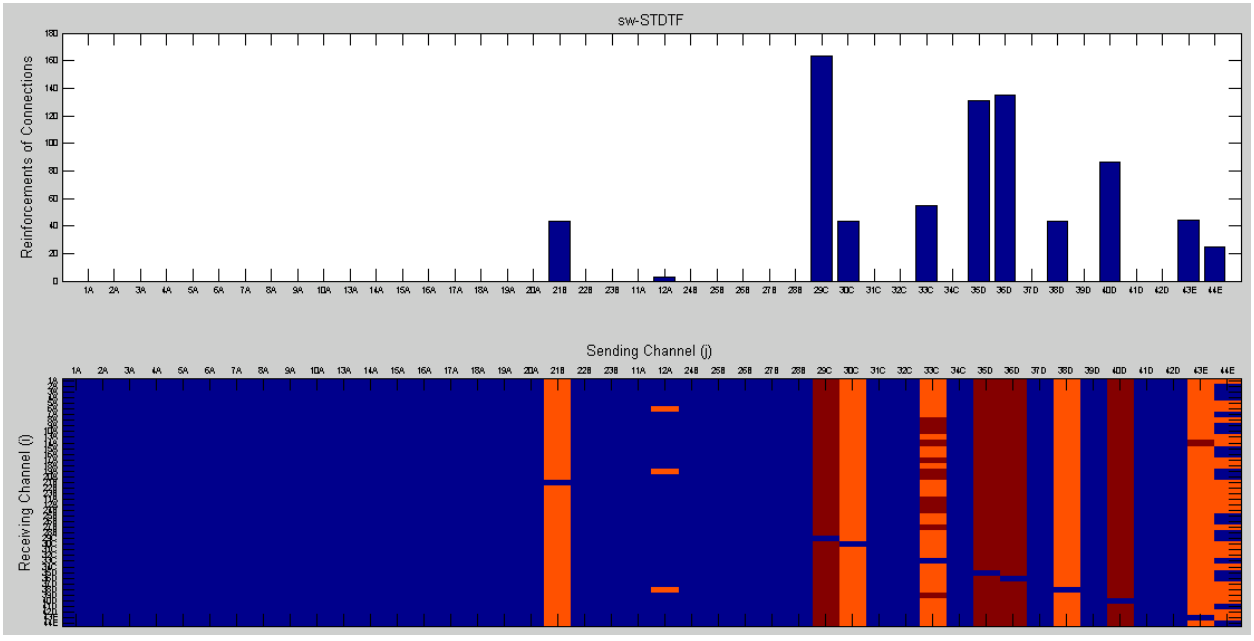

Seizure #6. Occurred at 6/13/2012 at 16:23:20. Electrographically, there was a subtle ictal pattern involving electrode contacts 2 through 6 on A grid over the left frontal head region. This was a subtle pattern and no clinical changes were noted during this event.

Adaptive Results:

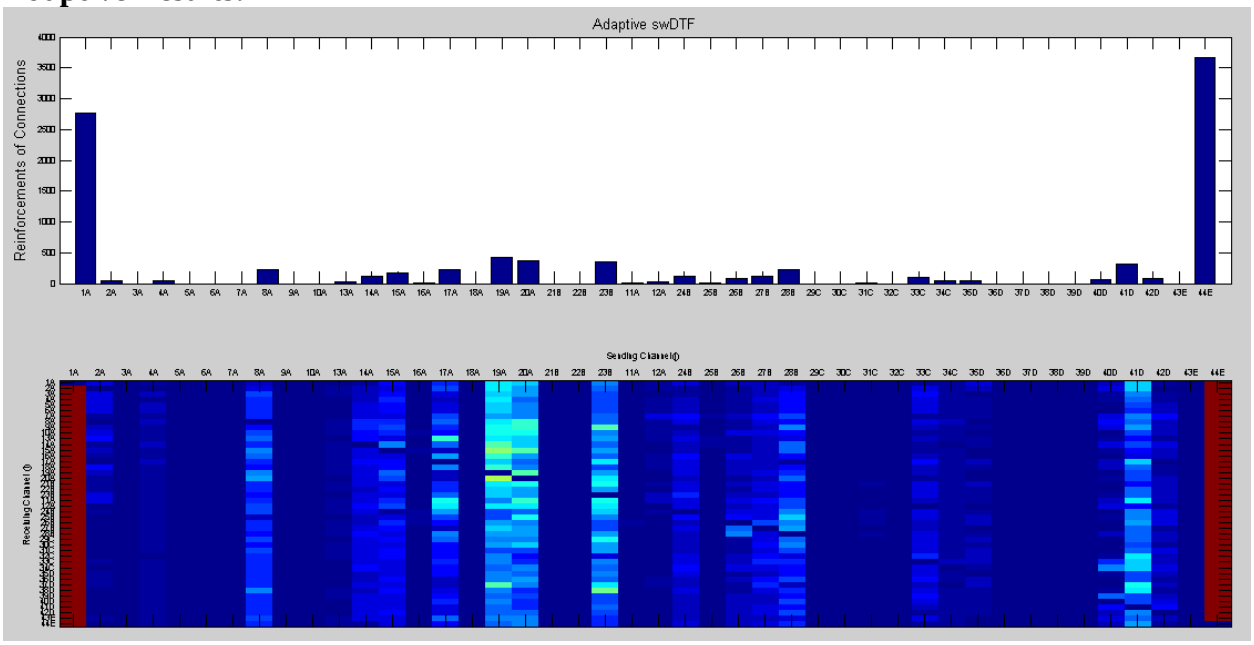

Short-Time Results:

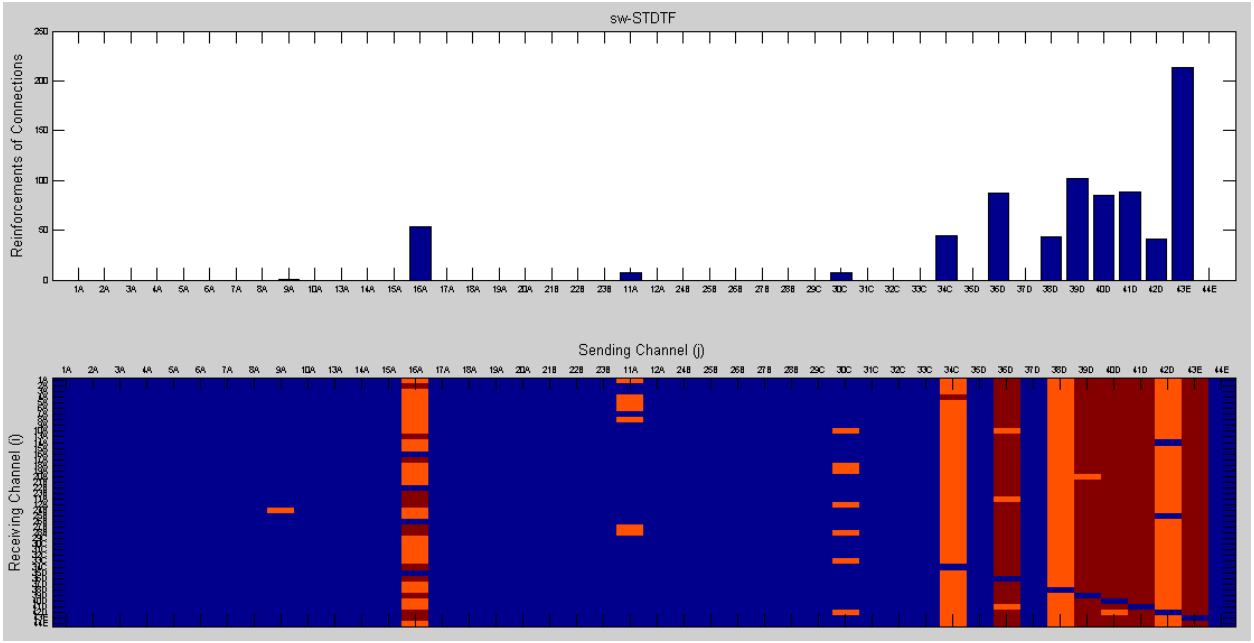

Seizure #7. Electrographically, at 16:47:57 on 6/13/2012 there was rhythmic sharply contoured theta activity over the left frontal grid (electrodes 2 through 6), which evolved into a spike configuration. This ictal pattern showed a subtle evolution before stopping at 16:49:24. Clinically, no clinical changes were noted on review of the video files.

Adaptive Results:

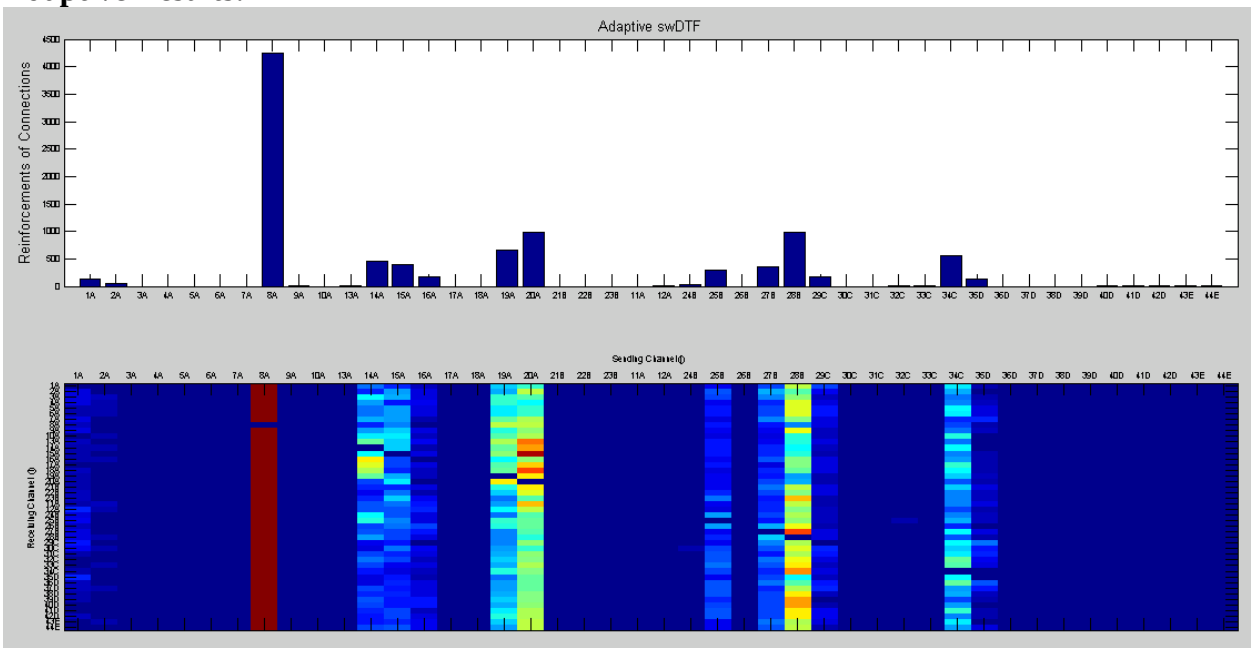

Short-Time Results:

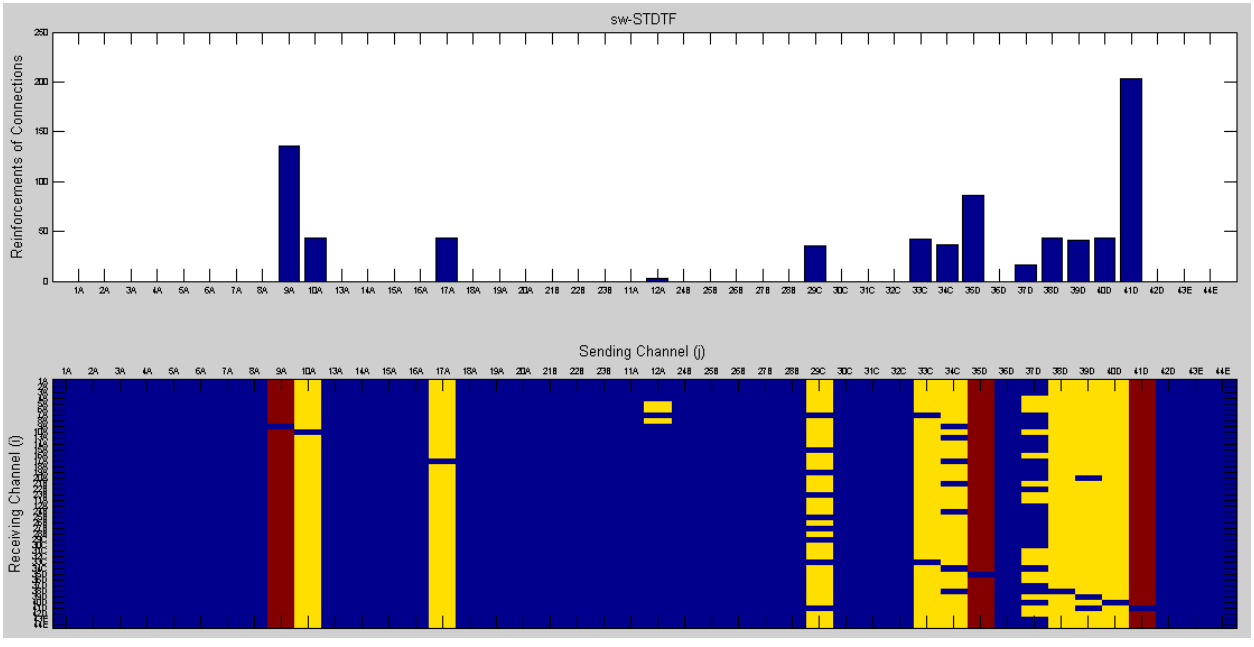

Seizure #8. Electrographically, a rhythmic, sharply contoured theta pattern was noted over the left frontal grid at 17:04:36. This evolved similar to seizure #7, evolving to a spike-like configuration before spontaneously terminating at 17:05:36. There appeared to be a field involving electrode 62, which was over the right basal frontal area. Clinically, no definitive changes were noted in the patient's behavior.

Adaptive Results:

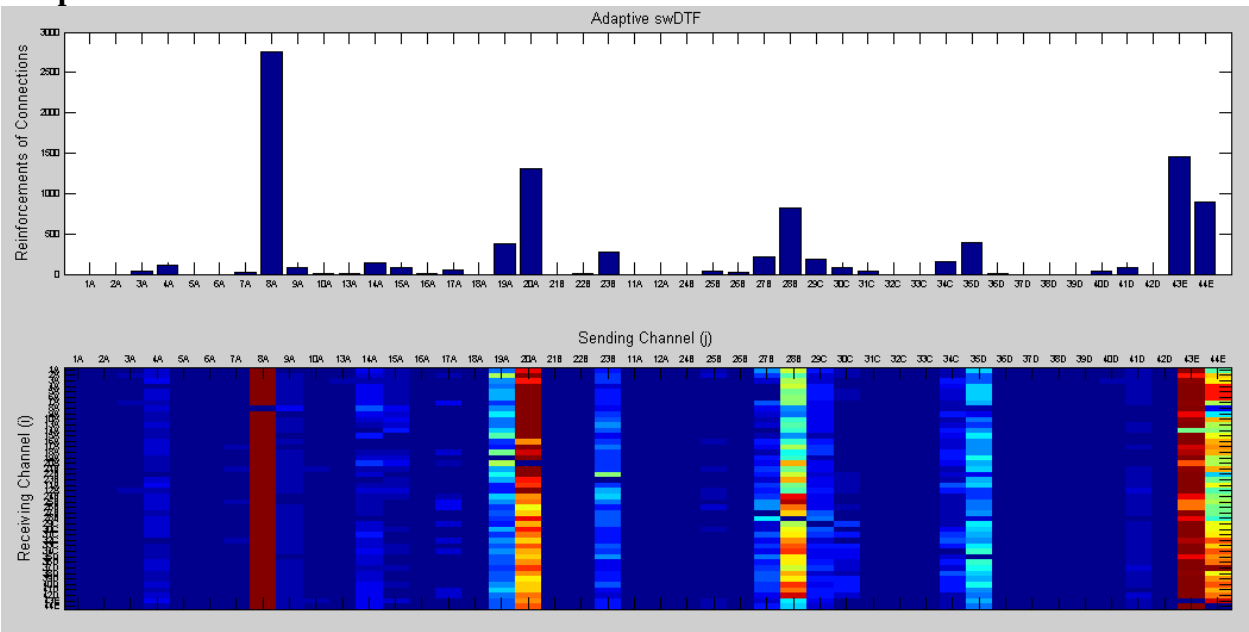

Short-Time Results:

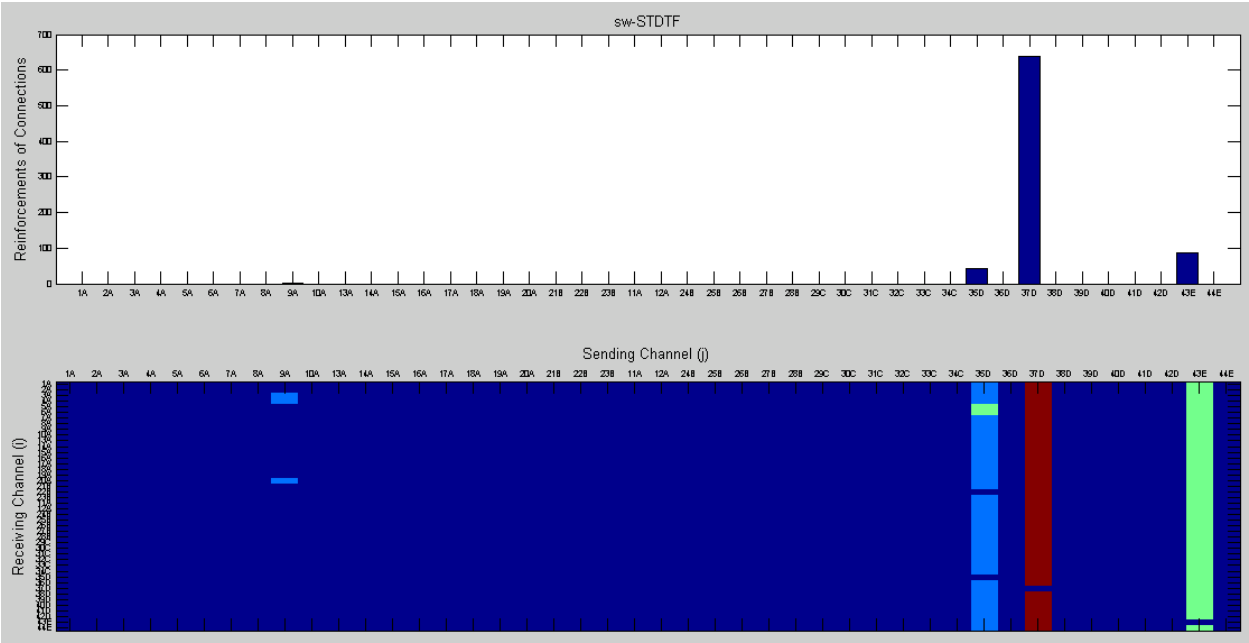

Seizure #9. Electrographically, at 22:13:44 on 6/13/2012, a beta buzz was noted. Within 2 seconds, this evolved to a 4-6 Hz spike-like pattern, maximum at electrodes 40-42. This evolved, becoming higher amplitude and slower in frequency before spontaneously terminating at 22:14:45.

Adaptive Results:

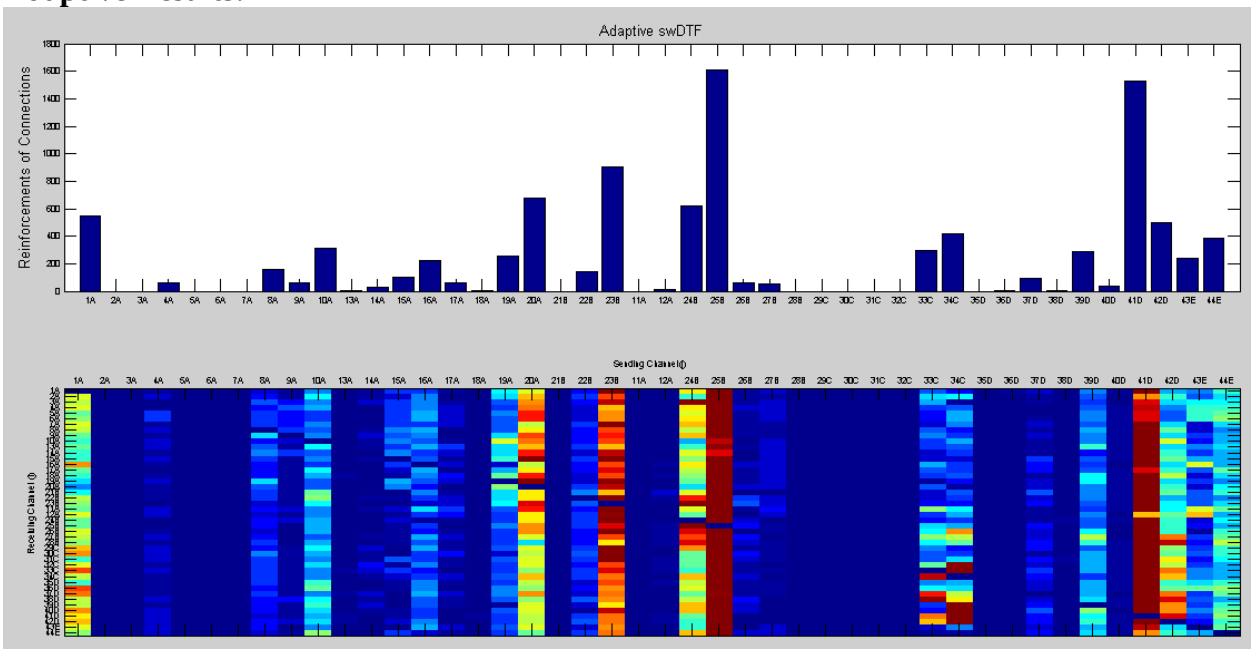

Short-Time Results:

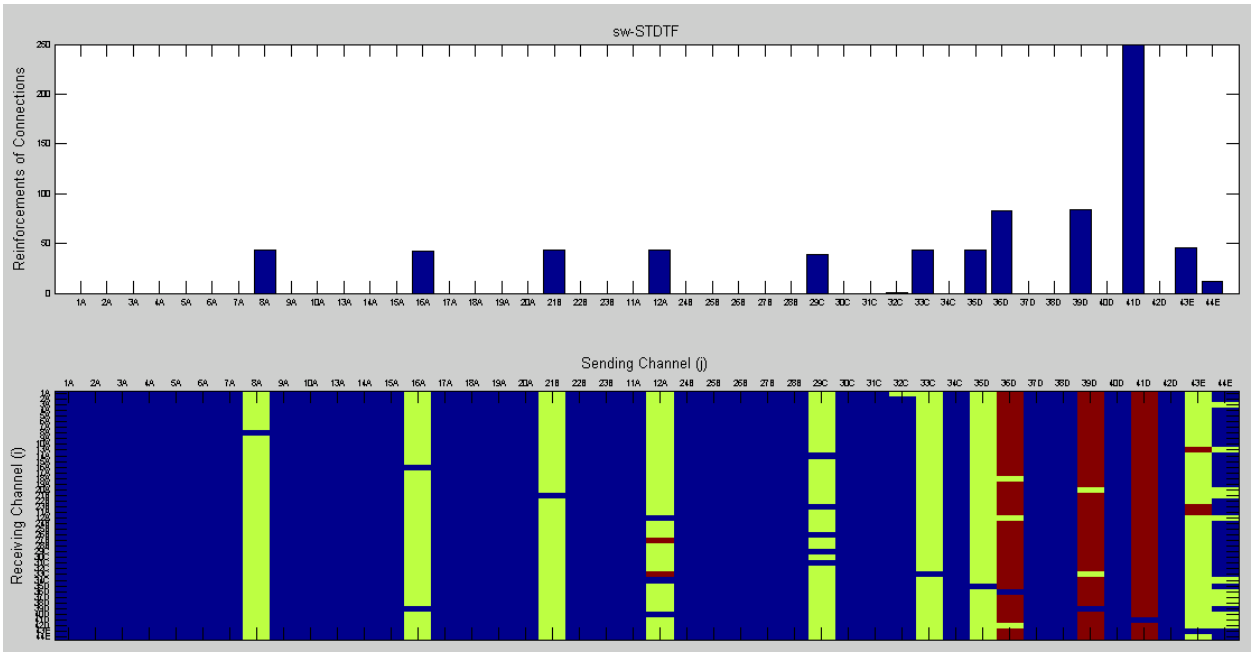

Seizure #10. Electrographically, at 00:05:14 on 6/14/2012, a beta buzz was noted. This evolved into repetitive 4 Hz spike-wave pattern involving electrodes 36, 42, and 44. This subsequently showed propagation and diffuse slowing over the frontal head regions, including the left frontal grid and the left interhemispheric strip. This spontaneously terminated at 00:07:26.

Adaptive Results:

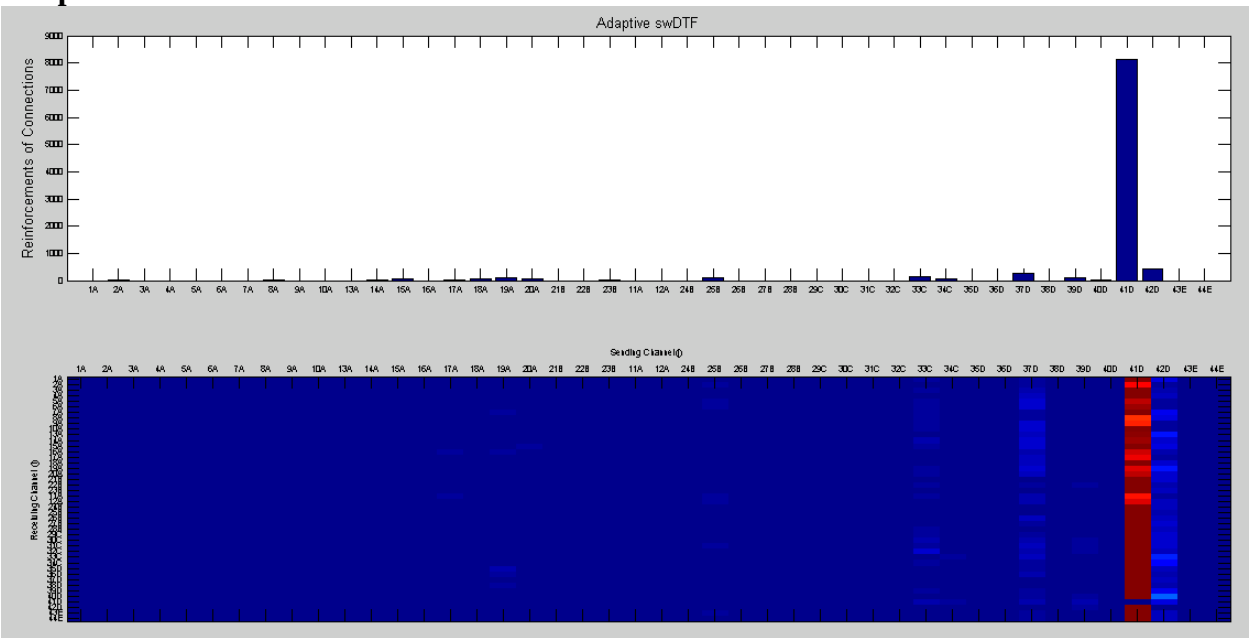

Short-Time Results:

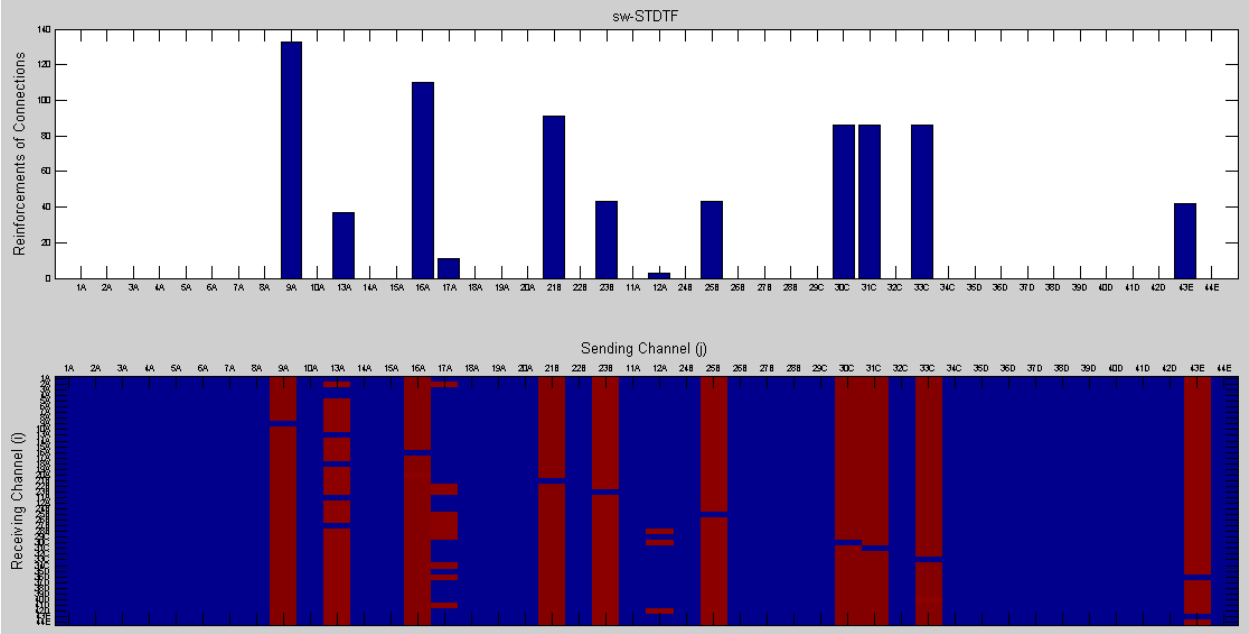

Seizure #11. Electrographically, a beta buzz was identified at 21:56:45 involving electrode contacts 33-34 and 35-42. This evolved into higher amplitude of 4-5 Hz spike and spike-wave pattern. Initially, this became a higher amplitude and slower frequency before spontaneously terminated at 21:57:54.

Adaptive Results:

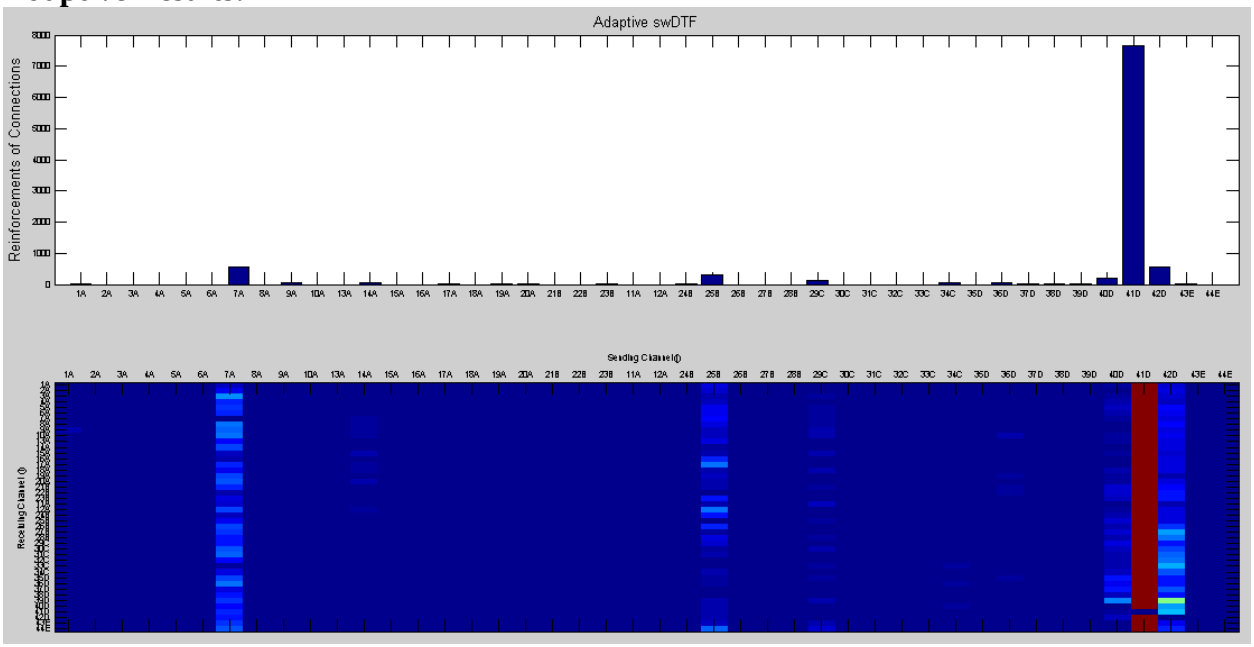

Short-Time Results:

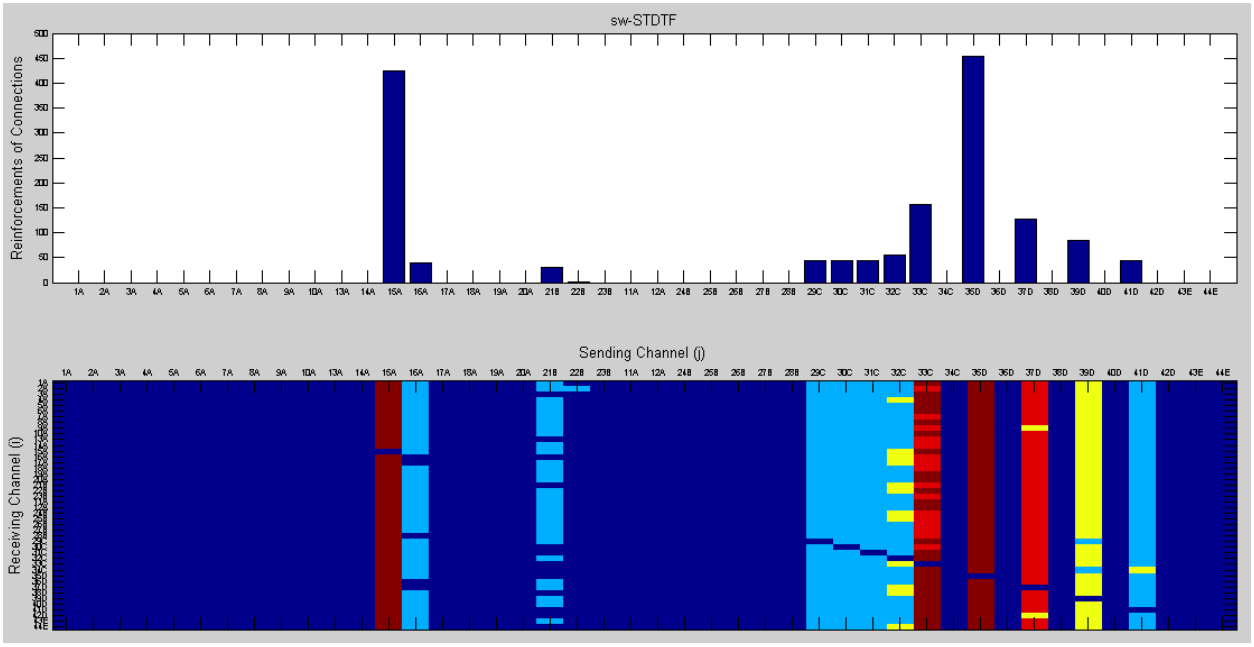

Seizure #12. Electrographically at 08:24:22 on 6/16/2012, a repetitive spike discharge was noted at 08:24:22, maximum at electrode contacts 34 and 41. This changed into a beta buzz at 08:24:25 and then evolved into a higher amplitude repetitive spike pattern initially in the theta range. This evolved becoming higher in amplitude and slower in frequency before spontaneously terminating at 08:25:35.

Adaptive Results:

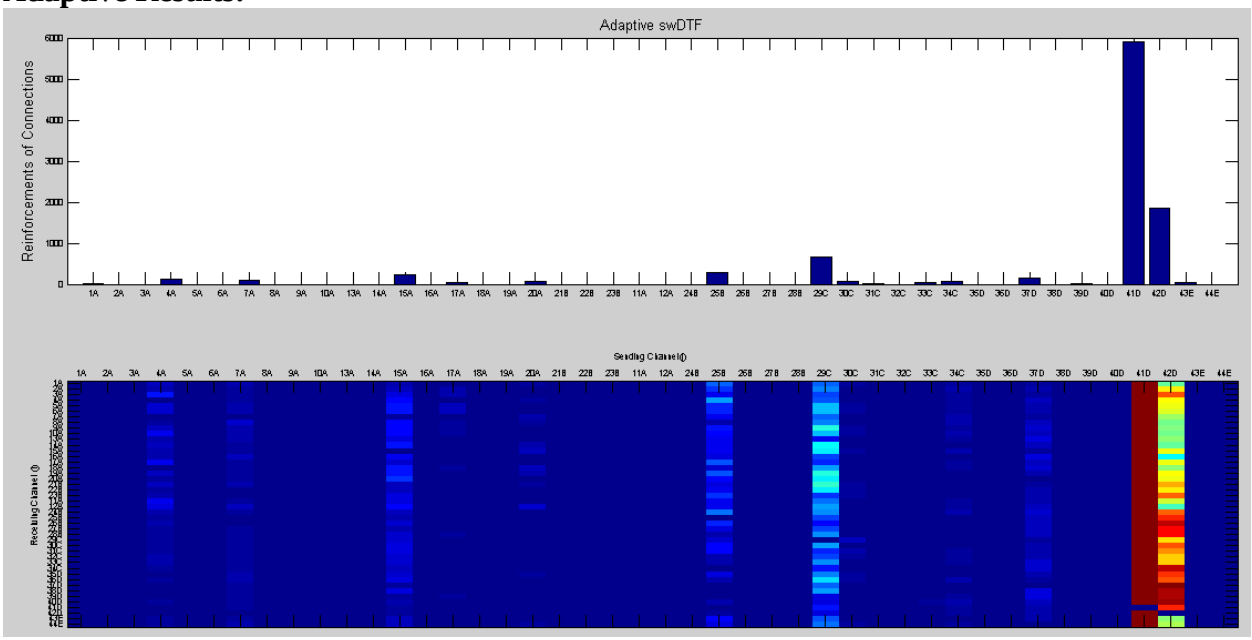

Short-Time Results:

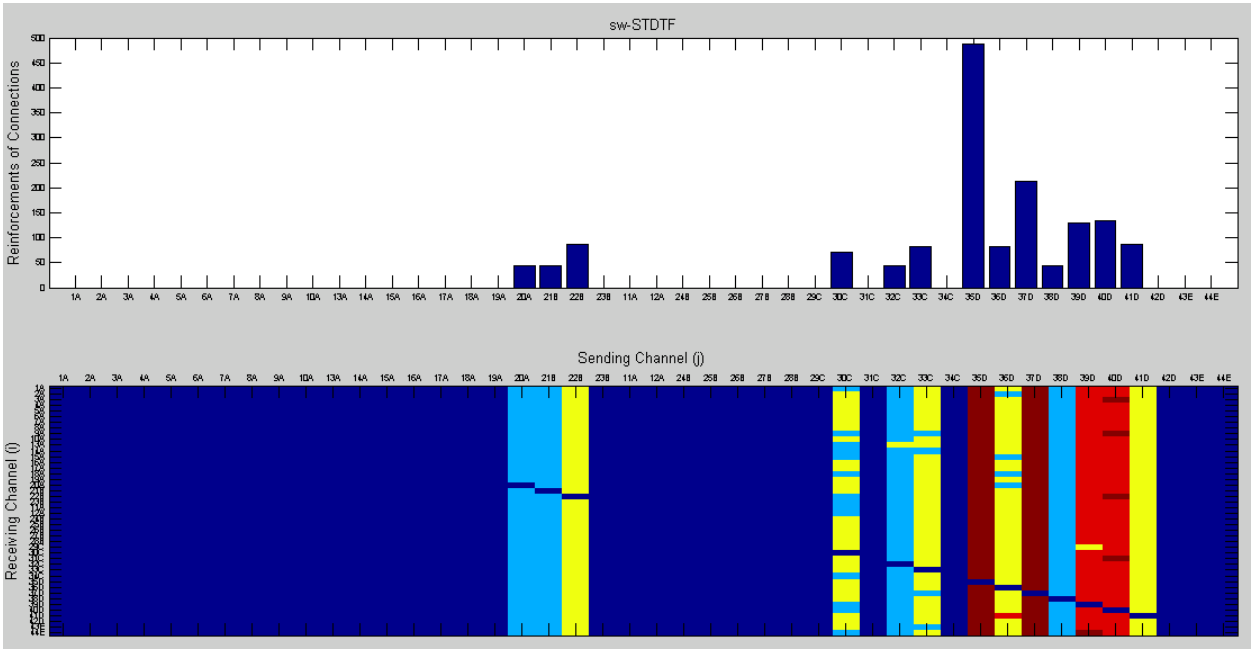

Seizure #13. Electrographically, at 05:26:06 on 06/17/2012, a beta buzz was recorded over electrode contacts 34 and 40. This evolved with subsequent spread to the frontal head regions at 05:26:50. This showed a similar electrographic evolution as previously noted in both subclinical events. This spontaneously terminated at 05:30:50.

Adaptive Results:

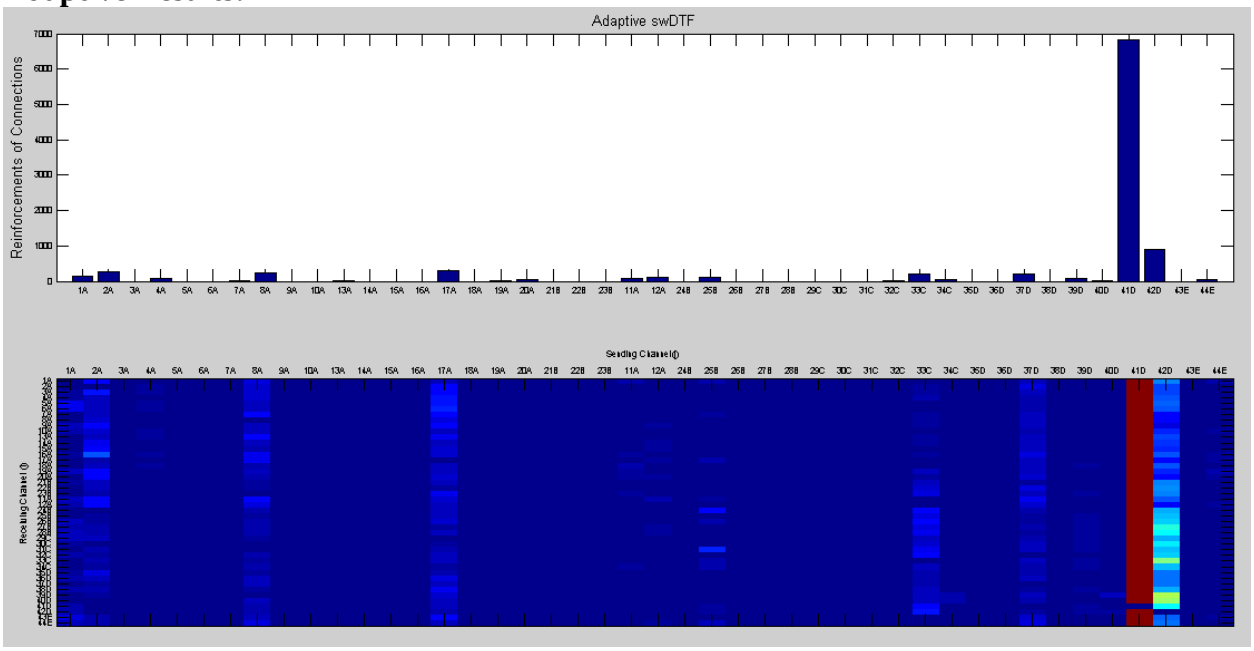

Short-Time Results:

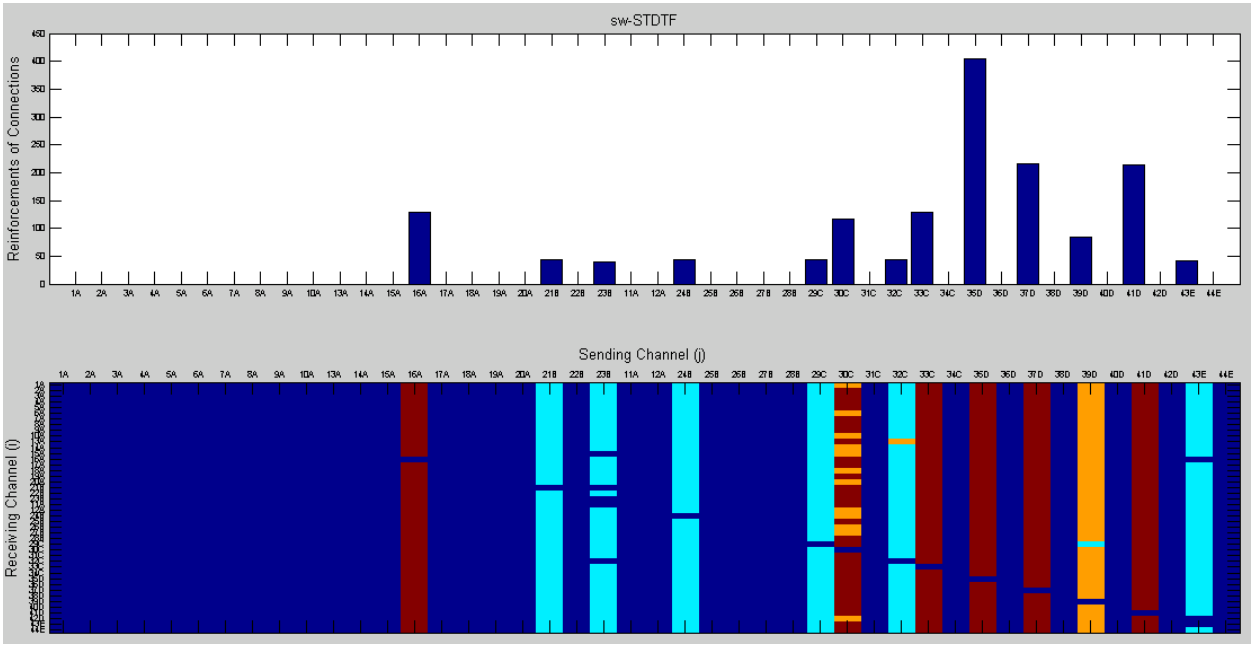

Seizure #14. Electrographically, a beta buzz was noted at electrodes 34 and 40 at 08:16:14. This evolved similar to previous documented ictal patterns. It showed spread to the frontal head regions at 08:16:54 and then secondary generalization at 08:24:06.

Adaptive Results:

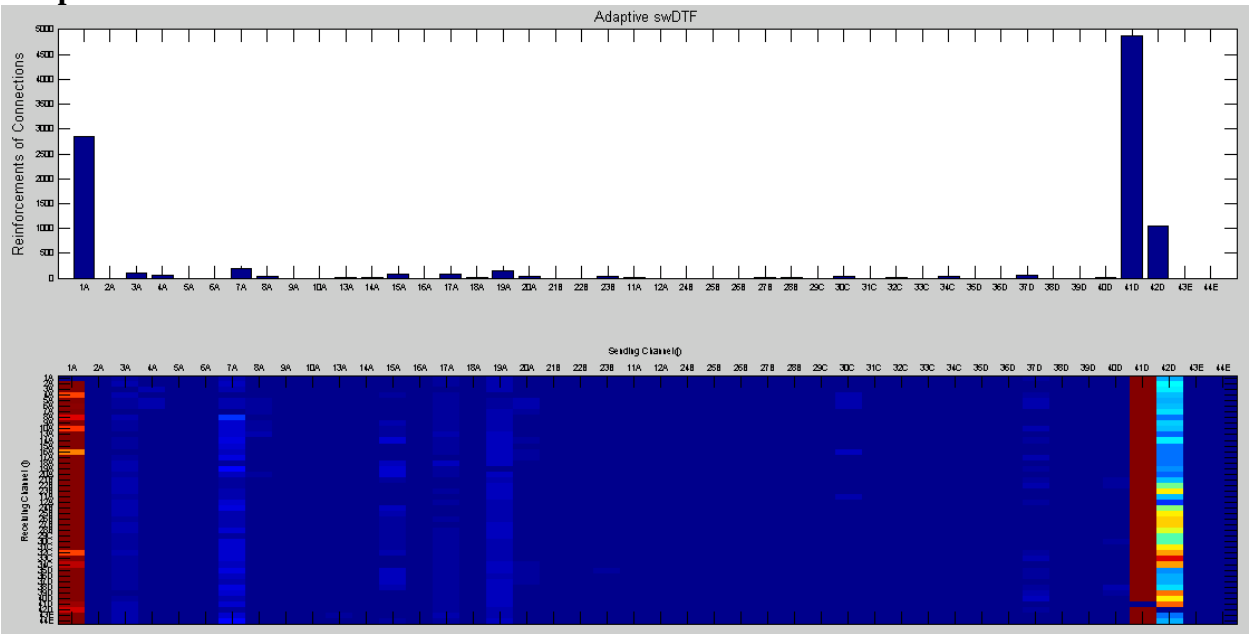

Short-Time Results:

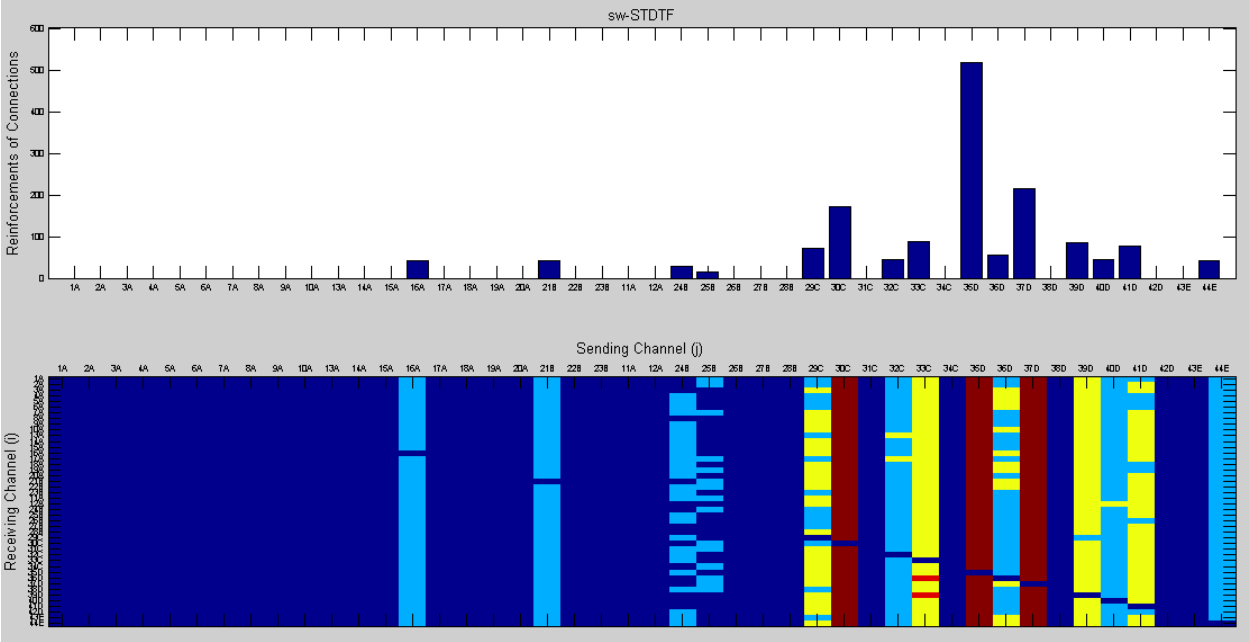

Seizure #15. Electrographically at 09:13:15 on 6/17/2012, repetitive spikes were noted at contacts 34 and 40. This evolved into a beta buzz at 09:13:21. This evolved, becoming higher amplitude and slower in frequency before terminating at 09:15:47.

Adaptive Results:

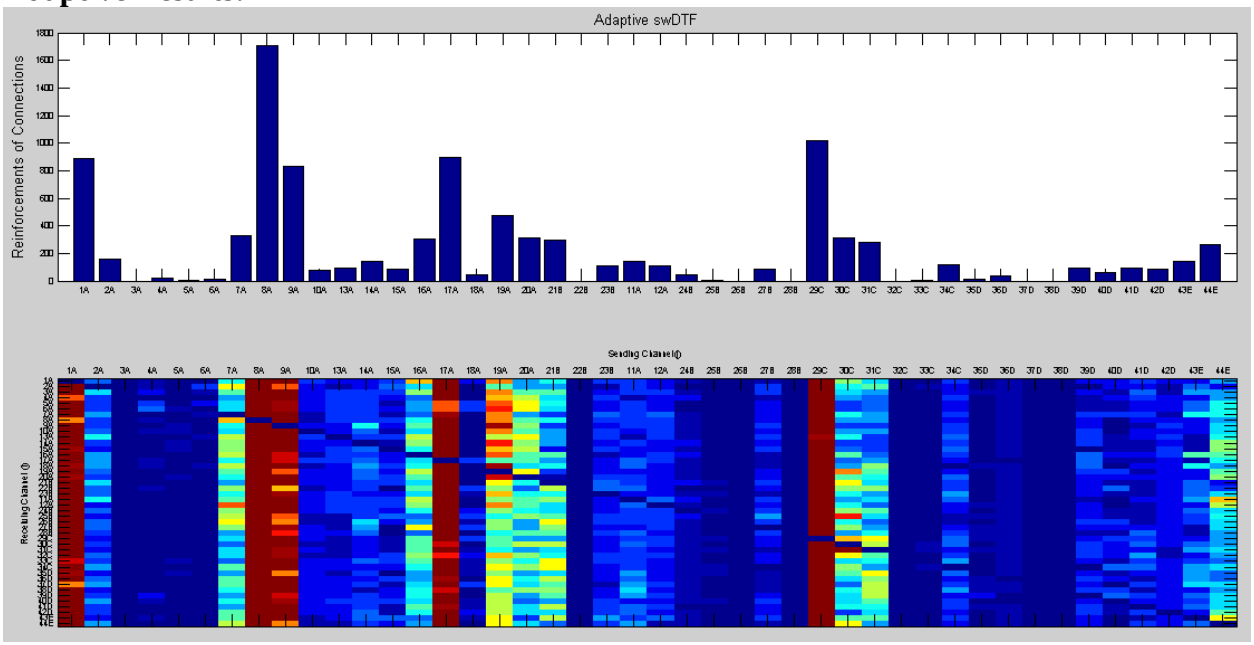

Short-Time Results:

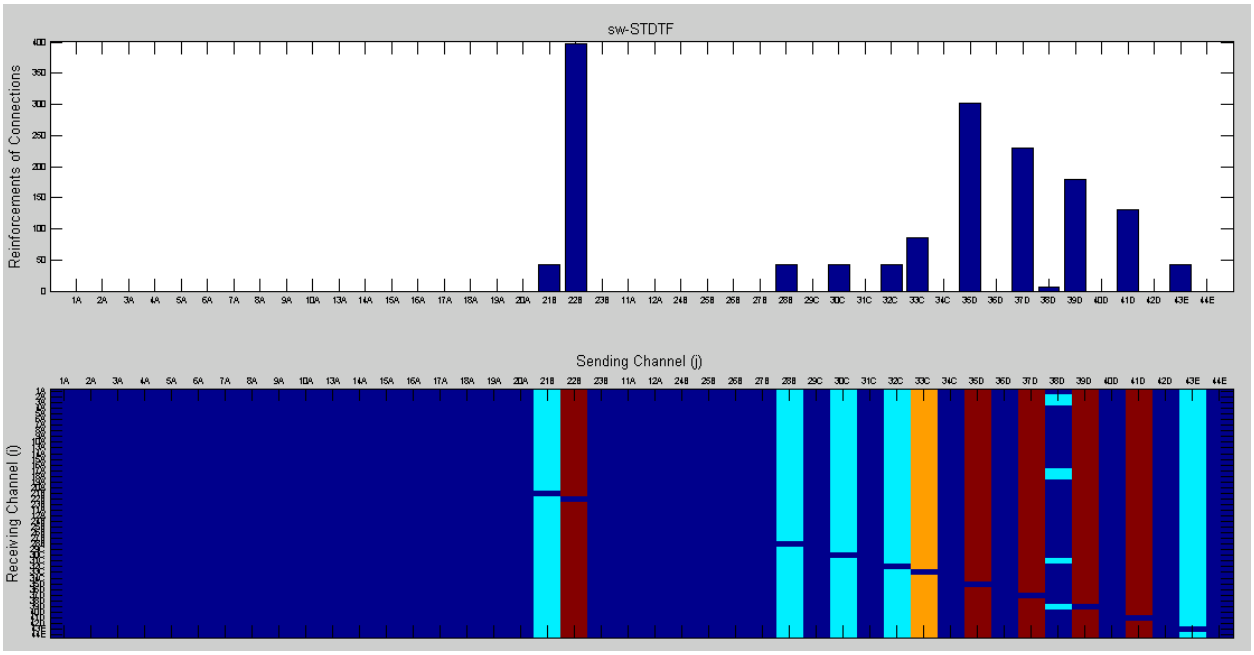

Subject 1:

Seizure 1: Occurred on 6/8/2012 at 23:21:29. In this event, rhythmic activity begins at 23:21:29 in the form of 4 Hz to 5 Hz slowing in contacts 51-55. Electrical activity evolves to high-frequency beta activity in contacts 51-53 from 23:21:34 to 23:21:36. By 23:22:03, polyspike and slow-wave activity is seen in contacts 26, 36, and 51-55. The event ends electrically at 23:23:08 with suppression of electrical activity, but the suppression is most prominent in contacts 51-55.

Adaptive Results:

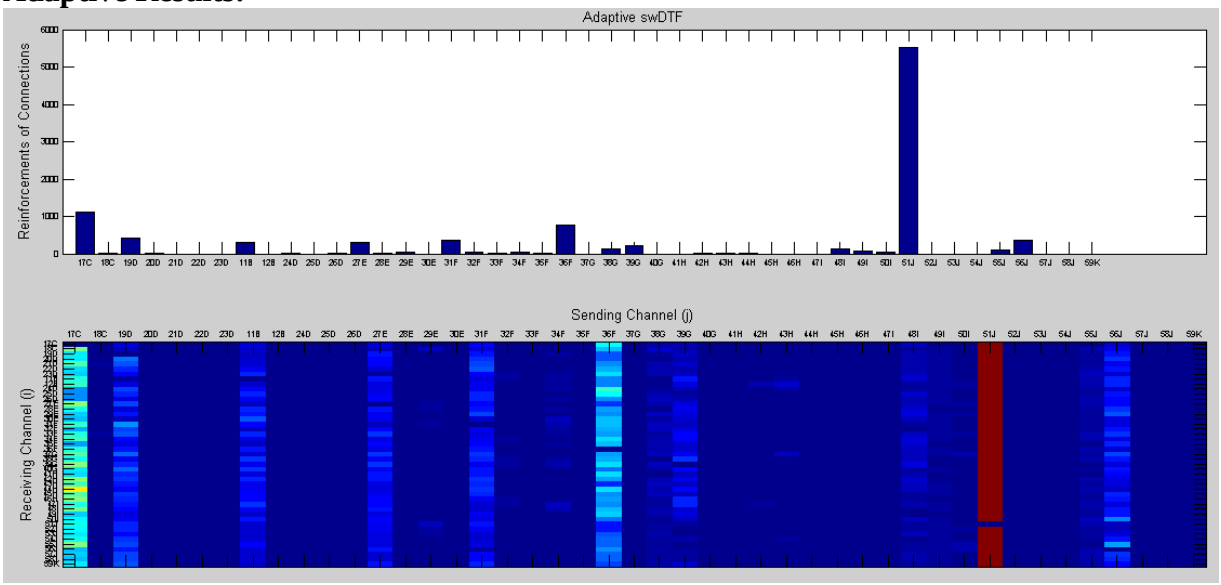

Short-Time Results:

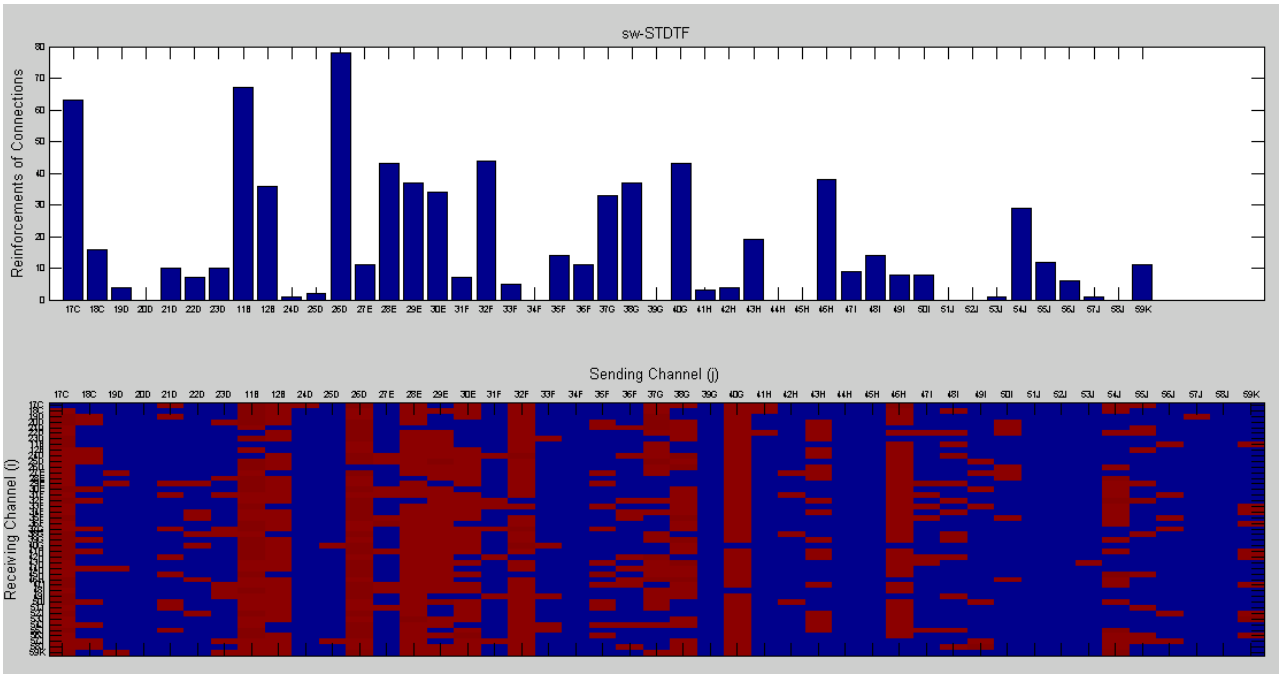

12. Appendix C: MATLAB Code

Main: Adaptive *swDTF*

```
%*************************************************************************
%*************************************************************************
% This program calculates the swADTF using the data from the EMU.
% Kalman filtering is used to estimate the multivariate
% time-varying autoregressive coefficients.  The time-varying transfer
% matrix is calculated and normalized to the swADTF.  A uniform threshold
% is set as the 99.9 percentile of the swADTF values and the number of
% connections based on the threshold is determined for each channel.  The
% measure outputs a bar graph showing the total connections for each
% channel as well as an image plot showing the various connections of each
% channel.  The channel with the highest connections is indicative of the
% epileptogenic focus.
%
% James Gurisko - Created: 7/16/2013
%               Last Updated: 4/16/2014
%*************************************************************************
%*************************************************************************
clear all;
%%%%%%%%%%%%%%%%%%%%%%%%%%%%%%%%%%%%%%%%%%%%%%%%%%%%%%%%%%%%%%%%%%%%%%%%
%%%%%%%%%%%%%%%%%%%%
%*************************************************************************
% USER: SET PARAMETERS HERE

File = 'DataNotes.xlsx'; %Name file with seizure #'s, start/stop times, etc
Dir = 'C:/eegData/SH-EEG/'; %Directory containing Patient data
Seizure = 1;%Which seizure to analyze (according to seizure # in File above)
len = 20;%Length of data to analyze (s)
Fs = 1000;%Sampling Frequency of data (Hz)
lchan = 1; hchan = 46; %Range of channels to analyze (e.g. 1-46)
%*************************************************************************
%%%%%%%%%%%%%%%%%%%%%%%%%%%%%%%%%%%%%%%%%%%%%%%%%%%%%%%%%%%%%%%%%%%%%%%%
%%%%%%%%%%%%%%%%%%%%

%Initialize reads in start/stop times of the seizure from File and converts
%them to absoulte points to be used in selecting the data to be analyzed.
%It also creates a vector of strings including the filename that will be
%used to import the data

%File = 'DataNotes.xlsx'; Dir = 'C:/eegData/SH-EEG/'; %Patient 2
%File = 'DataNotes_Patient1.xlsx'; Dir = 'C:/eegData/Subject 1 Data/'; %Patient 1
[Start_Vector, File_String] = Initialize(File,Dir);

%Open eeglab and import EDF data
%Seizure = 1; len = 20; %Seizure #, Length of desire signal in seconds
EEG = Import_EEG(Seizure,File_String);


%Select portion of data to analyze and normalize it
%lchan = 1; hchan = 46; %Patient 2
%lchan = 15; hchan = 61; %Patient 1
[y,xlabels] = extract_EEG(EEG,Fs,Seizure,Start_Vector,len,lchan,hchan);
```

```
% %Decimate the data
dF = 4; %1000/4 = 250Hz
[x,fs,n,m] = decimate_EEG(y,Fs,dF); Fs = fs;

%CREATE MVAAR MODEL
%**************************************************************************
p = 10; UC = 0.001; N = 30; %P = model order, UC = update coefficient
disp('Creating MVAAR model...');
[H,S,F2] = mvaar_H_S(x',p,fs,N,UC);

%CALCULATE SWADTF & UNIFORM THRESHOLD
%**************************************************************************
%Form is: swADTF(i,j,t);
f1 = 5; f2 = 30; %Frequency limits to compute over
[swADTF, UTsw] = calc_swADTF(H,f1,f2);

% Calculate Connections based on Threshold across all n
%**************************************************************************
[ConnOutsw,Connsw] = calc_conns(swADTF,UTsw,m,n);

% Plot histogram and output image
%**************************************************************************
subplot(2,1,1);
bar(Connsw,'stacked');title('Adaptive swDTF');ylabel('Reinforcements of Connections');
set(gca,'XTick',[1:size(x,1)]);set(gca,'XTickLabel',...
   xlabels(1:size(x,1)));set(gca,'FontSize',6);
subplot(2,1,2);
image(((ConnOutsw./max(max(ConnOutsw))).*255));set(gca, 'XAxisLocation', 'top');
set(gca,'XTick',1:size(x,1));set(gca,'XTickLabel',xlabels(1:size(x,1)));
set(gca,'YTick',1:size(x,1));set(gca,'YTickLabel',...
   xlabels(1:size(x,1)));set(gca,'FontSize',6);ylabel('Receiving Channel (i)');
   xlabel('Sending Channel(j)');
% %**************************************************************************
% %**************************************************************************
```

Main: Short-Time *swDTF*

```
%*************************************************************************
%*************************************************************************
% This program calculates the swST-DTF using either the data from the
% simulation or Spectrum Health's EMU.
% Short-Windows are used to generate a time dependant version of the DTF.
% This is normalized to the spectrum-weighted ST-DTF (swST-DTF)
%
% James Gurisko - Created: 11/11/2013
%                 Updated: 4/16/2014
%                 **This is a modification to the swADTF Kalman Fitler
%                 approach for delineating the epileptogenic focus for my
%                 thesis
%*************************************************************************
%*************************************************************************
clear all;
%%%%%%%%%%%%%%%%%%%%%%%%%%%%%%%%%%%%%%%%%%%%%%%%%%%%%%%%%%%%%%%%%%%%%%%%
%%%%%%%%%%%%%%%%%%%%
%*************************************************************************
% USER: SET PARAMETERS HERE

File = 'DataNotes.xlsx'; %Name file with seizure #'s, start/stop times, etc
Dir = 'C:/eegData/SH-EEG/'; %Directory containing Patient data
Seizure = 1;%Which seizure to analyze (according to seizure # in File above)
len = 20;%Length of data to analyze (s)
Fs = 1000;%Sampling Frequency of data (Hz)
lchan = 1; hchan = 46; %Range of channels to analyze (e.g. 1-46)
%*************************************************************************
%%%%%%%%%%%%%%%%%%%%%%%%%%%%%%%%%%%%%%%%%%%%%%%%%%%%%%%%%%%%%%%%%%%%%%%%
%%%%%%%%%%%%%%%%%%%%

%Initialize reads in start/stop times of the seizure from File and converts
%them to absoulte points to be used in selecting the data to be analyzed.
%It also creates a vector of strings including the filename that will be
%used to import the data

%File = 'DataNotes.xlsx'; Dir = 'C:/eegData/SH-EEG/'; %Patient 2
%File = 'DataNotes_Patient1.xlsx'; Dir = 'C:/eegData/Subject 1 Data/'; %Patient 1
[Start_Vector, File_String] = Initialize(File,Dir);

%Open eeglab and import EDF data
%Seizure = 1; len = 20; %Seizure #, Length of desire signal in seconds
EEG = Import_EEG(Seizure,File_String);



%Select portion of data to analyze and normalize it
%lchan = 1; hchan = 46; %Patient 2
%lchan = 15; hchan = 61; %Patient 1
[y,xlabels] = extract_EEG(EEG,Fs,Seizure,Start_Vector,len,lchan,hchan);

% %Decimate the data
dF = 4; %1000/4 = 250Hz
[x,fs,n,m] = decimate_EEG(y,Fs,dF); Fs = fs;
```

```
%Short-Time Directed Transfer Function (ST-DTF)
%*************************************************************************
win_len = Fs/10;  %Length of Window
overlap = fix(win_len*0.5); %Amount of overlap
[M,N]=size(y); %Number of channels and samples
Nf = Fs/5; %Number of frequency points
Fmax = 30; %Max freq limit in DTF calculation

%Determine optimal order for AR model
[w,A_TI, C_TI, sbc, fpe, th] = arfit(y',1,20,'sbc');
[tmp, p_opt] = min(sbc); p_opt = 4;

disp('Generating Short-Time MVAR Model');
% ST_DTF = zeros(M,M,Nf,ceil(len/win_len));
start = 1; i = 1;
while(start + win_len - 1 < N),
   y_part = y(:,start:start+win_len-1)';
   y_win = y_part.*repmat(hamming(size(y_part,1)),1,M);
   [A,RCF,PE] = mvar(y_win,p_opt,7);
   ST_DTF(:,:,:,i) = DTF_matrix(A,p_opt,Fs,Fmax,Nf);
   start = start + (win_len-overlap);
   i = i + 1;
end

%CALCULATE SWSTDTF & UNIFORM THRESHOLD
%*************************************************************************
%Form is: swADTF(i,j,t);
f1 = 5; f2 = 30; %Frequency limits to compute over
[swSTDTF, UTsw] = calc_swADTF(H,f1,f2);

% Calculate Connections based on Threshold across all n
%*************************************************************************
[ConnOutsw,Connsw] = calc_conns(swSTDTF,UTsw,m,n);

% Plot histogram and output image
%*************************************************************************
subplot(2,1,1);
bar(Connsw,'stacked');title('Short-Time swDTF');ylabel('Reinforcements of Connections');
set(gca,'XTick',[1:size(x,1)]);set(gca,'XTickLabel',...
   xlabels(1:size(x,1)));set(gca,'FontSize',6);
subplot(2,1,2);
image(((ConnOutsw./max(max(ConnOutsw))).*255));set(gca, 'XAxisLocation', 'top');
set(gca,'XTick',1:size(x,1));set(gca,'XTickLabel',xlabels(1:size(x,1)));
set(gca,'YTick',1:size(x,1));set(gca,'YTickLabel',...
   xlabels(1:size(x,1)));set(gca,'FontSize',6);ylabel('Receiving Channel (i)');
   xlabel('Sending Channel(j)');
% %*************************************************************************
% %*************************************************************************
```

Functions:

```
function [Start_Vector, File_String] = Initialize(file,dir)
%This program initializes the swADTF_measure by performing
%the following options:
%       - Adding Necessary Paths
%       - Opening file containing start stop times of seizure
%       - Reading in .EDF file names
%
%The function returns the vector of Seizure Start times and the vector
%containing the full strings of the file name that can be used to load
%the data into EEGLAB
%
% Inputs:
% file = name of xlsx file containing start/stop times of seizure
%         e.g. 'DataNotes.xlsx'
% dir = directory containing EEG files
%         e.g. 'C:/eegData/SH-EEG/'
%
% Outputs:
% Start_Vector = Start times of each seizure in absoulte points
% File_String = Vector of strings containing full file name w/ path
%*************************************************************************
%Add necessary folders
addpath('C:/eegData/MATLAB/Guriskoj','C:/eegData/MATLAB/WOSSPA_Mathworks_v2',...
    'C:/eegData/MATLAB/eeglab10.2.2.4b');

%Read in start times of seizure
Hour = xlsread(file,1,'O:O');
Minute = xlsread(file,1,'P:P');
Second = xlsread(file,1,'Q:Q');

%Calculate absolute start in terms of sample number per file
Start_Vector = (((Hour.*60)+Minute).*60)+Second;

%Read in filenames
[num FileNames raw] = xlsread(file,'I:I');
size(FileNames)
clear num; clear raw;

%Create full string to used to import data
for b = 1:1,
    File_String(b,1) = strcat(dir, FileNames(b+1,1));
end


function [EEG] = Import_EEG(b,File_String)

%This program imports the .EDF EEG file using EEGLAB and biosig toolbox and
%returns the EEG structure
%
%
% Inputs:
% b = Seizure number to import (from 'datanotes.xlsx')
```

```
% Start_Vector = vector of start times of seizures
% File_String = vector containing file name + directory
%        e.g. 'C:/eegData/SH-EEG/BA26802N_1-1.edf'
% dt = time segment to import (e.g. 20 seconds)
%
% Outputs:
% EEG = Strucutre of imported .edf file
%*************************************************************************
eeglab; %Open EEGLAB
FileTemp = File_String(b);
FileFinal = FileTemp{1};
EEG = pop_biosig(FileFinal,'importevent','off','blockepoch','off');

EEG.setname='CurrentSet';
EEG = eeg_checkset( EEG );
eeglab redraw;

function [x2,xlabels] = extract_EEG(EEG,Fs,b,Start_Vector,dt,lchan,hchan)
%This function extracts the portion of data that will be analyzed from the
%complete two hour segment of EEG data.  The function extracts the data
%from Start to Stop for all channels between lchan and hchan (low channel
%and high channel).  The function also creates a vector of containing the
%electrode label of the extracted channels.
%
%The function also normalizes the data using the zscore
%
% Inputs:
% EEG = EEG struct returned by EEGLAB, used for getting Channel Labels
% Fs = Decimated Sampling Frequency
% b = Seizure number
% Start_Vector = Vector of start times from Initialize function
% dt = time segment to import (e.g. 20 seconds)
% lchan = Low end channel to include in analysis
% hchan = high end channel to include in analysis
%
% Outputs:
% x = Extracted Data of size hchan:lchan by Start*Fs:Stop*Fs
%*************************************************************************
y = EEG.data; y = double(y);

Start = Start_Vector(b); Stop = Start+dt;

%Constant, identifies EEG Mark channels to remove
eegmark1 = 39; eegmark2 = 40;

%Take channels lchan-hchan (except 39, 40 which are "EEG marks")
%Take 20 seconds of data, 5 before onset, 15 after
x(1:length(lchan:(eegmark1-1)),:) = y(lchan:eegmark1-1,Fs*Start:Fs*Stop - 1);
x(length(lchan:(eegmark1)):hchan-lchan-1,:) = y(eegmark2+1:hchan,Fs*Start:Fs*Stop - 1);

%Create channel labels vector of channels used in measure
xlabels_temp = char(EEG.chanlocs.labels); xlabels = xlabels_temp;
xlabels(1:length(lchan:(eegmark1-1)),:) = xlabels_temp(lchan:eegmark1-1,:);
xlabels(length(lchan:(eegmark1)):hchan-lchan-1,:) = xlabels_temp(eegmark2+1:hchan,:);
xlabels = cellstr(xlabels);
```

```
%Normalize mean and standard deviation
x2 = zscore(x,0,2); %Standardize across rows

function [y2,fs,n,m] = decimate_EEG(y,Fs,dF)
%This function decimates each channel of the EEG data by the downsample
%factor and returns the decimated data and the new sampling frequency
%
% Inputs:
% y = (double) EEG.data
% Fs = Initial Sampling Frequency (Hz)
% dF = Downsample factor (e.g., fs = 1000/dF = 1000/4 = 250 Hz)
%
% Outputs:
% y2 = Decimated data
% fs = New sampling frequency
% n = New number of samples
% m = Number of channels
%*************************************************************************
fprintf('Decimating the data by a factor of %d...',dF);

fs = round(Fs/dF); %Calculate decimated sampling frequency

for i = 1:size(y,1),
   ytemp = decimate(y(i,:),dF);
   y2(i,:) = ytemp(1,:);
end
[m,n]=size(y2);

function [H,S,f] = mvaar_H_S(X,p,fs,N,UC)
% Returns time variant, frequency-dependent transfer and spectral matrices,for an adaptive MVAR model
% of order p fit to the n-by-m signal X, where n is the number of time values and m is the number
% of channels.
% fs = sampling frequency
% N = number of evenly spaced frequency values from 0 to fs/2.

% Outputs:
% f= frequency vector.
% H= m by m by n by N by n transfer matrix. H(i,j,F,t) denotes the transfer
% function from i to j at time t, frequency F.
% S= spectral density matrix of dimension m by m by N by n.
[n,m]=size(X);
f = (0:N-1)*(fs/(2*N));
[x,e,Kalman,Q2] = mvaar(X,p,UC);
%       A: stores the autoregression coefficients and is of size n by p*m*m,
%       where rows correspond to time, and columns correspond to
%       autoregressive coefficients. For example, if p=3 (model order) and
%       m=4 (channels) and there are n=50 time observations, then A has 50 rows and
%       3*4*4=48 columns. The first m*m=16 columns correspond to the
%       autoregressive coefficient, A1, the second m*m=16 columns correspond
%       to the autoregressive coefficient, A2, and so on, up to Ap.
%       e: n by m matrix of process noise vectors, having covariance matrix
%       Sigma
%Sigma=cov(e);size(e);
```

```
H=zeros(m,m,N,n);
S=zeros(m,m,N,n);
disp('Done with mvaar function')
for t=1:n
   for F=1:N
      A0=eye(m,m);
      Asum=A0;
      for j=1:p
         Aj=zeros(m,m);
         for k=1:m
            Aj(k,:)=x(t,1+(k-1)*p*m+(j-1)*m:(k-1)*p*m+j*m);
         end;
         Asum=Asum-Aj*exp(-sqrt(-1)*2*pi*j*F*1/fs);%use Asum -

      end;
      Y=inv(Asum);
      H(:,:,F,t)=Y(:,:);
      S(:,:,F,t)=H(:,:,F,t)*Q2(:,:,t)*ctranspose(H(:,:,F,t));S(:,:,1,10);
   end;
end;

function [swADTF, UT] = calc_swADTF(H,f1,f2)
%Returns the spectrum-weighted Adaptive Directed Transfer Function values
%from the transfer function matrix coefficients and the Uniform Threshold
%value to use for counting the number of connections.  The uniform
%threshold is set to the 99th percentile of the swADTF values
%
% Inputs:
% H = transfer function matrix of form H(i,j,f,t)
% f1 = lower frequency band to compute swADTF
% f2 = upper frequency band to compute swADTF
%
% Outputs:
% swADTF = spectrum-weighted Adaptive Directed Transfer Function values of
% form swADTF(i,j,t)
%*************************************************************************
disp('Calculating swADTF...');
[m, m2, N, n] = size(H);
swADTF = zeros(m,m,n); swADTF_noDiag = swADTF;
for i = 1:m,
   i
   for j = 1:m,
      Ksum(1,:,:) = sum(abs(H(j,:,f1:f2,:)).^2,2);
      Hsum_temp(1,:,:) = ((abs(H(i,j,f1:f2,:).^2)));
      Hsum(1,:) = sum(Hsum_temp.*Ksum,2);
      Ssum(1,:,:,:) = sum(abs(H(:,:,f1:f2,:)).^2,2);
      Ssum = reshape(Ssum, [ 1 m length(f1:f2) n]);
      Hsum2_temp(1,:,:,:) = abs(H(i,:,f1:f2,:)).^2;
      Hsum2(1,:,:) = sum(Hsum2_temp.*Ssum,3);
      Hk(1,:) = sum(Hsum2,2);
      swADTF(i,j,:) = Hsum(1,:)./Hk(1,:);
      swADTF_noDiag(i,j,:) = swADTF(i,j,:);
      if(i==j),
        swADTF_noDiag(i,j,:) = 0;
      end
   end
```

```
end
swADTF_noDiag = reshape(swADTF_noDiag, [1,m*m*n]);
UT = prctile(swADTF_noDiag,99.9)

function [ConnOutsw, Connsw] = calc_conns(swADTF,UTsw,m,n)
%Returns the number of "connections" for each relationship of channels
%summed across all time based on the uniform threshold.  ConnOutsw is a mxm
%matrix consisting of the total number of connections for each pair of
%channels over all time. It also creates the histogram for by summing
%across all channels for each channel
%
% Inputs:
% swADTF = spectrum-weighted adaptive-directed Transfer Function
%          swADTF(i,j,t)
% UTsw = value of the uniform threshold (calculated as 99.9 percentile in
%        calc_swADTF function
% m = number of channels (will automate so you don't have to pass this)
% n = length of signal (will automate so you don't have to pass this)
%
% Outputs:
% ConnOutsw = mxm matrix of total number of "connections" for each pair of
%             channels across all n time points
% Connsw = 1xm vector representing histogram of connections for each
%          channel
%*************************************************************************
ConnOutsw = zeros(m,m);
%Calculate connections
for TO = 1:m,
   for FROM = 1:m,
      %Grab all time points for particular TO/FROM channel combination
      swADTF_temp = swADTF(TO,FROM,:);
      %Reshape temporary swADTF to vector
      swADTF_temp = reshape(swADTF_temp,[1 n]);
      %UTsw_temp = UTsw(FROM,TO)
      for T = 1:n,
         if ((swADTF_temp(1,T)>=UTsw)&&(TO~=FROM)),
            %Increment Output connecs for each time exceeding threshold
            ConnOutsw(TO,FROM) = ConnOutsw(TO,FROM) + 1;
         end
      end
   end
end
%Create histogram
%Sum connections for each channel for histogram
Connsw = zeros(1,m);
z = 0;
for j = 1:m,
   z = z + 1;
   for i = 1:m,
      Connsw(1,z) = Connsw(z) + ConnOutsw(i,j);
   end
end
```